TECHNICAL AND VOCATIONAL TRAINING INSTITUTE (TVTI)

School of Graduate Studies

FACULTY OF ELECTRICAL AND ELECTRONICS TECHNOLOGY AND INFORMATION AND COMMUNICATION TECHNOLOGY (DEPARTMENT OF ELECTRICAL AND ELECTRONICS TECHNOLOGY)

Induction motor control for a long-range drive of an Electric Vehicle with three single-phase H-bridge inverters by using PI controller

MSc Thesis for the Partial Fulfillment of

Master of Science in Electrical Automation and Control Technology Management

By,

Alemu Aragaw Kasahun (MTR/441/13)

Supervisor,

Dr. Bisrat Gezahagn

AUGUST 2022

Addis Ababa, Ethiopia

Induction motor control for a long-range drive an Electric Vehicle with three single-phase H-bridge inverters by using PI controller

A Thesis submitted to

TECHNICAL AND VOCATIONAL TRAINING INSTITUTE (TVTI)

FACULTY OF ELECTRICAL AND ELECTRONICS TECHNOLOGY AND INFORMATION AND COMMUNICATION TECHNOLOGY (DEPARTMENT OF ELECTRICAL AND ELECTRONICS TECHNOLOGY)

In partial fulfillment for the Degree

MASTER OF SCIENCE *in* ELECTRICAL AUTOMATION AND CONTROL TECHNOLOGY MANAGEMENT

By,

Alemu Aragaw Kasahun (MTR/441/13)

Supervisor,

Dr. Bisrat Gezahagn

DECLARATION

I hereby declare that the work which is being presented in this thesis entitled" Induction motor control for a long-range drive an Electric Vehicle with three single-phase H-bridge inverters by using PI controller" is the original work of my own, has not been presented for a master's thesis in this or other universities and all sources of materials used for this thesis work have been fully acknowledged.

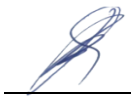
Name: - Alemu Aragaw Kasahun (MTR/441/13)

Signature: _____

Place: Addis Ababa

Date of Submission: _____

This thesis proposal has been submitted for examination with my approval as a TVTI advisor.

Dr. Bisrat Gezahagn		Sept.9,2022
Name	Signature	Date

TECHNICAL AND VOCATIONAL TRAINING INSTITUTE (TVTI)
FACULTY OF ELECTRICAL AND ELECTRONICS TECHNOLOGY AND INFORMATION AND COMMUNICATION TECHNOLOGY
(DEPARTMENT OF ELECTRICAL AND ELECTRONICS TECHNOLOGY)

Thesis on

Induction motor control for a long-range drive Electric Vehicle with three single-phase H-bridge inverters by using PI controller

By,
Alemu Aragaw Kasahun (MTR/441/13)

APPROVED BY THESIS ADVISORY COMMITTEE

Name of the Advisor	Signature	Date
Dr. Bisrat Gezahagn	----------	Sept. 9, 2022
Name of Examiner Exsternal	Signature	Date
Dr. Mengesha Mamo	----------	Sept. 7, 2022
Name of Examiner, Internal	Signature	Date
Dr. Yohans Haylemeskel	----------	----------
Name of Chairperson	Signature	Date
Mr. Zemenu Tamir	----------	----------

DEDICATION

I dedicate this thesis to my family, who have always supported me in my studies and kept me safe.

I dedicate this thesis to everyone who has helped me along the road, including my adviser, instructors, friends, and coworkers. I will always be grateful for everything they have done.

ACKNOWLEDGMENTS

First and foremost, I want to express my gratitude to the Almighty God for giving me all I have and for making my studies go as smoothly as it has.

Second, I want to sincerely thank my adviser, Dr. Bisrat Gezahagn, for his important counsel, insightful criticism, supportive words, ongoing direction, inspiration, excitement, and vast knowledge. His advice was helpful to me during the whole thesis-writing process.

Last but not least, I want to thank my department's professors, my family, and my friends for their unending love and support all year long. Throughout my graduate studies, they increased my enthusiasm and determination.

ACRONYMS AND ABBREVIATIONS

i_{as}, i_{bs}, i_{cs}	Three phase stator current
$i_{ds}*$	D axis stator current
$i_{qs}*$	Q axis stator current
T_d	Developed torque
T_d*	Reference Developed torque
λ_r	Rotor flux vector
λ_r*	Reference of Rotor flux vector
AC	Alternative current
BEV	battery electric vehicles
BMS	Batter management system
CMV	common-mode voltage
DC	Direct current
DC	Direct current
EV	Electric Vehicles
HEB	Hybrid electric vehicles
i_Ds and *i_Qs*	Q component of stator current
LQR	linear quadratic regulator
MLI	multilevel inverter
MOSFETs	Metal oxide semiconductor field effect transistor
OBC	observer based controller
OEWIM	Open end winding induction
PI	Proportional integral
PID	Proportional-integral-derivative
PPC	pole placement controller
PR	Proportional resonant
PWM	Pulse width modulation
SPWM	Sinusoidal Pulse width modulation
SV	Space Vector
SVM	Space vector modulation
ZSV	zero-sequence voltage

ΔT_d	Torque error
$\Delta \lambda_r$	Flux error
λqm	q Axis air gap flux linkage
λdm	d Axis air gap flux linkage
ib,ic	Current supplied by inverter
ki	integral gain constant
ia , ib , ic	three phase motor currents (A)
kp	proportional gain constant
ia, ib, ic	Stator phase a, b, and c current (A)
i_{rq}, i_{rd}	Rotor q − and d − axis currents (A)
i_{sq}, i_{sd}	Stator q − and d − axis currents (A)
isq, isd	Stator q − and d − axis currents (A)
J	Combined inertia of motor and load (kgm^2)
L_{lr}	rotor leakage inductances (H)
L_{ls}	stator leakage inductances (H)
L_m	magnetize inductances (H)
L_q, L_d	q − and d − axis inductances (H)
L_r	rotor inductances (H)
L_s	stator inductances (H)
P	Number of pole pairs
R_r	Resistance of the rotor windings (Ohm)
Rr	Motor resistance (Ohm)
R_s	Resistance of the stator windings (Ohm)
Rs	Stator resistance (Ohm)
Te	Electromagnetic torque (Nm)
Tf	Motor shaft static friction torque (Nm)
Tm	Motor shaft torque (Nm)
v_a, v_b, v_c	Stator voltage phases a, b, c (V)A)
van, vbn, vcn	Stator phase a, b, and c voltage (V)
v_{sq}, v_{sd}	Stator q − and d − axis voltages (V)
Θ_{da}	dq stator electrical angle with respect to the rotor a − axis (rad)
Θ_{dA}	dq stator electrical angle with respect to the rotor A − axis (rad)
λ_{rq}, λ_{rd}	Rotor q − and d − axis flux (Wb)

λ_{sq}, λ_{sd}	Stator q − and d − axis flux (Wb)
ω_{da}	dq stator electrical speed with respect to the rotor a − axis (rad/s)
ω_{dA}	dq stator electrical speed with respect to the rotor A − axis (rad/s)
ωm	Angular mechanical velocity of the motor (rad/s)
ωm	Angular mechanical velocity of the rotor (rad/s)

Abstract

This thesis is concerned with the control of an induction motor for an Electric Vehicle (EV) with three single-phase H-bridge inverters. Nowadays the emission of carbon into the environment is a worldwide concern. In the industrial automobile process, the service of batteries for long-distance driving is always a challenge in the electric vehicle industry. This is due to the circulation of current in parallel configured batteries module. To tackle this problem three single-phase dc-link is proposed to supply the induction motor through the current controlled converter. Therefore, 21 battery cells are configured in series to achieve the dc-link voltage and 50 number of modules are configured to satisfy the current rating of the motor. Therefore, three Single-phases H- Bridge inverter is proposed to control the electric motor of EV and improve its performance. Each winding of the three-phase induction motor is connected with one single-phase H-bridge converter. The three-phase voltage and current are taken from the converter output and transformed to the dq at the synchronous reference frame. The life of the battery and stability of battery voltage is controlled by using proportional plus integral (PI). The circulation current that reduces the life and performance of the battery of the electric vehicle can be reduced by one-third as compared with the conventional three-leg common dc-link converters. The performance of an electric vehicle under its various modes of operation conditions is demonstrated and the simulations are carried out by Matlab/Simulink software.

***Keywords*:** Electric Vehicle, Induction Motor, PI, Open-ended winding induction motor and three single-phase H-bridge inverter

Table of Contents Page

DECLARATION i

APPROVAL SHEET ii

DEDICATION iii

ACKNOWLEDGEMENTS iv

ACRONYMS AND ABBREVIATIONS v

Abstract viii

Table of Contents ix

Lists of Tables xii

Lists of Figures xiii

CHAPTER ONE: INTRODUCTION 1

1.1 Bacground of the study 1

1.2 Statement of problem 4

1.3 Objective of the study 4

1.3.1 General objective 4

1.3.2 Specific objective 4

1.4 Scope of the thesis 5

1.5 Limitation of the thesis 5

1.6 Significance of the thesis 5

1.7 Organization of the study 6

CHAPTER TWO 7

LITERATURE REVIEW AND INDUCTION MOTOR OF ELECTRIC VEHICLE 7

2.1 Literature review 7

2.2 Recent works 7

2.3 Summary of literature 9

CHAPTER THREE: SYSTEM MODELING 10

3.1 Mathematical modelling of Induction Motor for electric vehicle 10

3.1.1 Electric motor Vehicles 10
3.1.2 challenge of electric vehicles 12
3.1.3 Induction motor modelling for EV 12
3.1.4 Three-phase asynchronous machine 21
3.1.5 Electrical System of the Wound-Rotor or Squirrel-Cage Machine 22
3.2 Power converter/inverter system design 23
3.2.1 Application of Inverters - 24
3.2.2 operation of single phase H-bridge Inverter.....24
3..3 Basic of power electronics control in Induction Motors.....24
3.3.1 power electronic - IGBT 25
3.3.2 Application of IGBT.....25
3.3.3 Principle Operation of IGBT 25
3.4 Modeling of H Bridge inverter Topology 25
3.4.1 H-Bridge inverter topology 25
3.4.2 Three single-phase H-Bridge Inverter 28
3.4.3 I/O and O/P specification for a system of electric vehicles 31
3.4.4 Electric motor sizing 34
3.5 Electric vehicle battery rating calculation.....35
3.5.1 EV design battery calculation 35
3.5.2 battery pack designs.....36
3.5.3 battery pack calculation.....37
3.6 voltage source inverter (VSI).....41
3.7 pulse width modulation (PWM).....43
3.7.1 Simulink model of unipolar pulse width modulation (PWM) 44
3.7.2 Sinusoidal pulse width modulation 44
CHAPTER 4: CONTROLLER DESIGN 48
4.1 Introduction.....48

4.2 System design 48
4.3 Controller 49
4.4 Design of PI Controllers 49
4.4.1 Proportional controller 50
4.4.2 Integral controller 51
4.4.3 PI controller 51
4.5 Ziegle-Nichols Tunning 53
4.5.1 Ziegler-Nichols first tunning method 53
4.5.2 Ziegler-Nichols second tunning method 54
CHAPTER 5: SIMULATION RESULTS AND DISCUSSION 55
5.1 subsystem of system design description 55
5.2 Stator voltage and current sensor 56
5.3 stator flux-based calculator 57
5.4 magnitude to angle subsystem 58
5.4.1 dq to abc conversation subsystem 59
5.5 current regulator subsystem 60
5.6 simulation result of the system design 60
5.6.1 PI controller performance of torque and flux 61
5.6.2 Three phase Current 61
5.6.3 Torque of the motor 61
5.6.4 Flux 62
5.6.5 Angle 63
CHAPTER 6: CONCLUSION AND FUTURE SCOPE 64
6.1 Conclusion 64
6.2 Future of the study 64
REFERENCE AND BIBLIOGRAPHY 65

List of tables

Table 3.1 Specifications and parameters for induction motor. 33
Table 3.2 The battery cells' input parameters. 37
Table 3.3 The energy density of each cell. 38
Table 3.4 The results of the equations aboves:. 40
Table 3.5 Switching conditions and on-status switches. 42
Table 3.6 Switching conditions and on-status switches 43
Table 4.1 Comparative study of the characteristics of a step response for a second order system for P and I controller.. 53
Table 4.2 Ziegler-Nichols Recipe – First Method. 54
Table 4.3 Ziegler Nichols Formula – Second Method 54

List of figures

Figure 1.1 Open-end winding induction motor drive was powered by three single-phase H-Bridge inverters. 3
Figure 3.1 Block diagram of power flow in an electric vehicle 11
Figure 3.2 Few electric vehicle models (photo courtesy Ford, Honda, Nissan, GM). 12
Figure 3.3 Fundamental Blocks/Machines.. 21
Figure 3.4 Q axis of asynchronous machine. 22
Figure 3.5 D axis of asynchronous machine.. 22
Figure 3.6 single phase H-bridge inverter.. 26
Figure 3.7 Structure of an H-bridge (highlighted in red).. 27
Figure 3.8 The two basic states of an H bridge 27
Figure 3.9 DC-AC conversion (voltage source inverter) for three phase 28
Figure 3.10 DC-AC conversion (voltage source inverter) for first phase 29
Figure 3.11 DC-AC conversion (voltage source inverter) for second phase 29
Figure 3.12 DC-AC conversion (voltage source inverter) for third phase 29
Figure 3.13 Proposed three single-phase H-Bridge inverters fed open-end winding induction motor drive 30
Figure 3.14 Schematic diagram of two-level VSI 42
Figure 3.15 Uni-polar PWM inverter for phase A 45
Figure 3.16 Uni-polar PWM inverter for phase B 45
Figure 3.17 Uni-polar PWM inverter for phase C 46
Figure 3.18 Unipolar PWM inverter waveforms output voltage and switching signals for phase A 46
Figure 3.19 Unipolar PWM inverter waveforms output voltage and switching signals for phase B 47
Figure 3.20 Unipolar PWM inverter waveforms output voltage and switching signals for phase C 47
Figure 4.1 Block diagram of direct vector control systems 48
Figure 4.2 Block diagram of PI controller 50
Figure 4.3 Proportional controllers in a feedback control loop. 50
Figure 4.4 Proportional gain block diagram 51
Figure 4.5 PI controllers in a feedback control loop. 53

Figure 5.1 Proposed PI control scheme for induction motor of electric vehicle and overall model of system design. 55
Figure 5.2 Flux and torque processor implementation. 57
Figure 5.3 Magnitude to angle conversation. 58
Figure 5.4 dq to abc conversation. 59
Figure 5.5 Current regulator. 60
Figure 5.6 Step responses of Three-phase current in (A). 61
Figure 5.7 Step responses of torque. 62
Figure 5.8 Step responses of flux. 63
Figure 5.9 Step responses of Angle. 63

CHAPTER ONE

INTRODUCTION

1.1 Background of the study

The automotive industry is currently making a major push into the electric drive sector. Several future car technology specialists have urged automakers to focus on new vehicle electric system designs and advancements. Several converters-fed motor drive systems with various power and speed ratings have become standard car features. For a number of factors, including as power conditioning, power control, and fuel efficiency, power converters are being employed more frequently in automobile applications [7]. These power converters have significant limits, much like any other embedded transportation system, particularly in terms of compactness and vehicle integration.

With the aim of reducing pollution and enhancing the driving experience, the popularity of electric vehicles (EVs) as a share of the commercial sector has increased in recent decades [25]. The electric motor at the center of an EV powers the wheels by converting electrical energy into mechanical energy [25]. In comparison to conventional internal combustion engines, electric motors have the advantages of being stronger, more energy-efficient, and more portable. It is preferable to produce lighter and more efficient electric motors to further increase the energy efficiency of modern EVs. Among all the popular EV motors, has drawn the most attention for its unique characteristics, which include a greater power-to-weight ratio, a smaller structure, high efficiency, particularly in multi-pole motors, high material usage, and improved performance of ventilation and cooling.

An inverter, also known as a DC-AC converter, is a device that converts a direct current input voltage into an alternating current output voltage with changeable amplitude and frequency [20]. Electric vehicles (EVs) in particular require a high level of availability (service continuity) [7]. The battery pack, inverter, and traction motor make up an EV's conventional drive train. The inverter, which is powered by the battery, powers the traction motor. A strong, high-density battery is necessary for an EV's extensive driving range. The battery's energy density is crucial. Electric vehicles frequently use lithium-ion batteries because of their high energy density and long lifespan.

It takes a number of series and parallel-coupled batteries to power an IM with a high power density, low line-to-line voltage, and high power. This combination makes maintaining constant potential across all battery connections challenging. A circulating current will flow between parallel batteries if their potentials are not equal, which could harm the battery and risk the stability and lifetime of the system. In battery-electric vehicles (BEV), lithium-ion batteries are now the most popular alternative. In a normal BEV battery pack, many cells, sometimes thousands, are linked in series and parallel to increase the pack's voltage, capacity, and current rating as needed. To lessen the quantity of parallel-connected batteries, an H-bridge inverter topology is offered. A single-phase H-Bridge inverter supplies electricity to each phase of the OEWIM [6]. This issue is addressed via battery equalization and a battery management system (BMS). To address the reported issue, a new distributed three single-phase H-Bridge inverter architecture is created using the PI controller technique. It has not yet been proposed to develop a three-phase H-bridge inverter for the induction motor of an electric vehicle (EV) controlled by a PI controller. So I'm interested in studying the design of the PI controller for three single-phase H-bridge inverters in an Electric Vehicle (EV). The suggested topology employs an open-end winding induction motor (OEWIM), with each phase fed by a single-phase H-Bridge inverter individually.

Mathematical models are utilized to better comprehend the behavior of induction motors in both transient and steady states. Dynamic modeling is used to determine all mechanical equations for inertia, torque, and speed vs. time. Additionally, it mimics every link between the stationary stator and the rotating rotor that has differential voltage, current, and flux. My mathematical model will depict a three-phase induction motor with transformations from three phases to d-q and d-q axis to three phases. It will be developed in MATLAB/Simulink. The key advantage of utilizing MATLAB, Simulink is that the equation in the mathematical model may be completed quickly and easily using function blocks.

This thesis is the fundamental building block of an H-bridge inverter. It features four switches, one for each phase. To fewer batteries being linked in parallel, a new distributed inverter topology is presented.. The analytical computation is performed to demonstrate one of the benefits of the suggested inverter topology.

In this study, It uses three single-phase H-Bridge inverters (namely, inverters A, B and C). Four discrete switches with the labels Sx1, Sx2, Sx3, and Sx4 are present in each single-phase H-Bridge inverter, where x is one of A, B, or C. A distinct stator phase winding is connected to each single-phase H-Bridge inverter. Vdc is equal to the DC-link voltage of each individual inverter. In order to reduce the parallel combination of batteries, this paper introduces three single-phase H-Bridge inverters that are powered by an OEWIM drive. SVMs are created using big and large vectors. To cut down on the number of batteries linked in parallel, a new distributed inverter topology is presented. The analytical computation is performed to demonstrate one of the benefits of the suggested inverter topology.

The figure 1.1 refers the individual phase winding motor phase voltage of an OEWIM drive that is provided by three single-phase H-Bridge inverters.

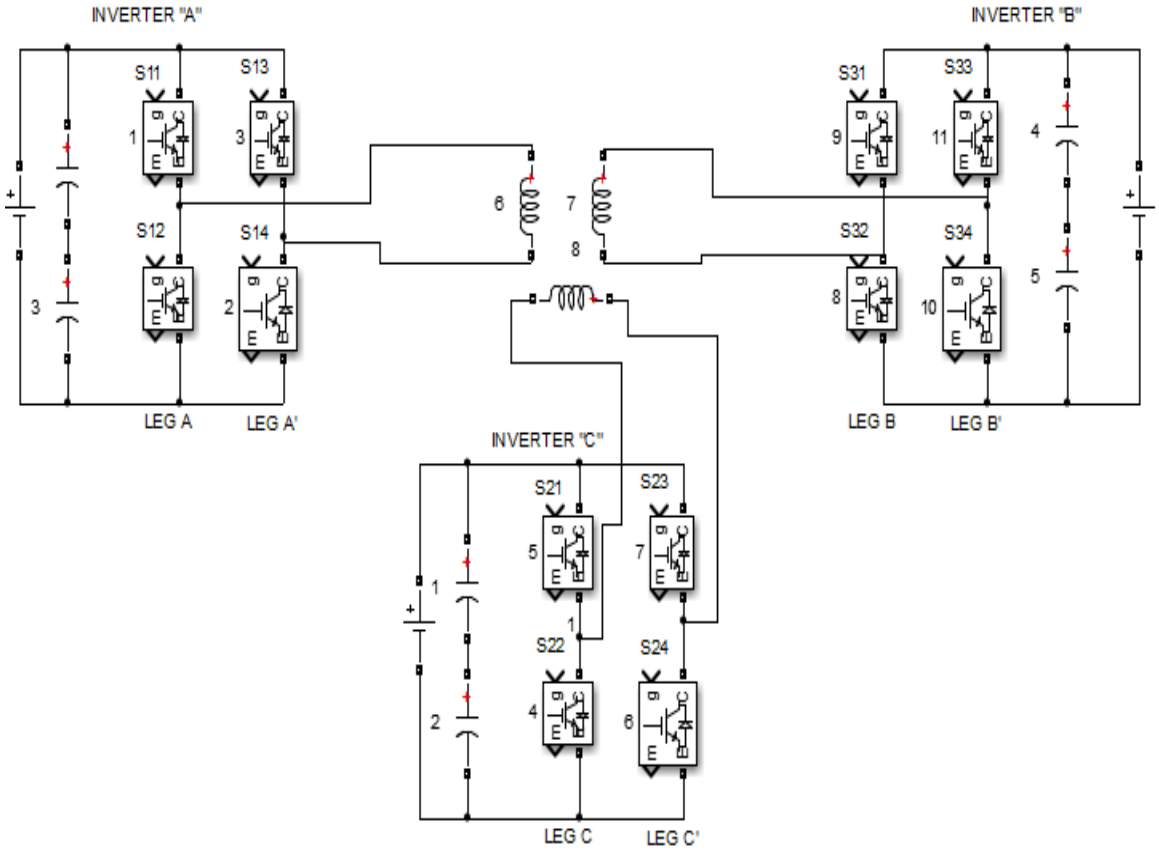


Figure 1.1 Open-end winding induction motor drive was powered by three single-phase H-Bridge inverters.

1.2 Statement of the problem

Designing and managing the voltage of the battery throughout a lengthy drive is one of the most common difficulties in the automobile business, particularly for an electric vehicle. The long-distance capability of an electric vehicle (EV) has been always a priority. To do this, a high-efficiency traction motor is used. Another alternative for increasing driving range is to connect more batteries in parallel. A large number of parallel-connected batteries, on the other hand, will result in circulating current in the battery circuit. The electric vehicle system's controlling premise is to manage the induction motor of an EV with consistent voltage throughout a long drive range. There are various options when the characteristics of batteries in an electric vehicle system change continuously, such as variation of battery volts over extended drives, which can disrupt vehicle speed. A proposed distributed three-phase H-Bridge inverter topology is being researched to solve this problem. In the topology under investigation, an open-end winding induction motor is used, and a single-phase H-bridge inverter supplies power to each phase of the winding. This decreases the number of batteries used in parallel.

Electric vehicles, on the other hand, must deliver high torque at zero speed, allow high-speed cruising (field weakening), and conserve battery energy by operating at a somewhat fluctuating DC battery voltage level. The potential system benefit analysis of the induction motor control for a long drive an electrical car with three single-phase H-bridge inverters using PI control approaches will be demonstrated in this thesis. The PI controller will control the inverter's switching state sequence. The PI controller strategy is used to control this system by switching three single-phase H-bridge inverters.

1.3 Objectives of the study

1.3.1 General Objective:

The overall purpose of this thesis is to use a PI controller to create control of an induction motor for a long-range drive of an Electric Vehicle (EV) with three single-phase H-bridge inverters.

1.3.2 Specific Objective

- ✓ To minimize the number of parallel connected battery cells used to generate a voltage for electric car motor drives.
- ✓ To increase the voltage stability of the motor drive and the battery's durability.

- ✓ To control the inverter voltage using PI approaches.
- ✓ Using the Matlab/Simulink toolbox, simulate and model the system controller.

1.4 Scope of Thesis

The power converter of an induction motor for electric vehicles, the PI control technique and a single-phase H-bridge inverter will be the only subject of this thesis research. Also, keep the number of battery cells linked in series and parallel to a minimum. This study, however, does not address all of the variables of induction motors and all of the components of electric vehicles. MatLab/Simulink simulation is used to validate the controller performance and switching of a single-phase H-bridge inverter.

1.5 Limitation of the thesis

The thesis is limited to induction motor modeling and controller simulation for long-range drive electric vehicle applications. As a result, the Matlab SIMULINK toolbox software will be utilized for data analysis and interpretation in order to investigate further information about electric vehicles.

1.6 Significance of the thesis

The main contribution of this thesis is the enhancement of the transient performance of an electric vehicle's induction motor. The PI controller's application is to tune the inverter line to line voltage. This thesis study made the following notable contributions:

- ✓ The PI controller is used to advance the transient and steady-state performance of a single-phase H-bridge inverter fed continuous voltage to an electric vehicle's induction motor.
- ✓ A lot of DC to AC conversion equipment depends on converters, including automated voltage regulator (AVR) systems, uninterruptible power supply (UPS), and induction motor drives.
- ✓ Alter the number of series-connected battery cells that produce DC voltage.

1.7 Organization of the study

The rest of the thesis is divided into five chapters. The following is an overview of the upcoming chapters:

Chapter two: discusses the literature of different scholars in the field of my studies like the article, journal paper, and conference and research paper related to the induction motor of EV and H-bridge inverters. It outlines the control schemes and focuses on the battery cell voltage generated in the induction motor of the EV system.

Chapter three: discusses the system modelling, mathematical modeling and Simulink of a system further.

Chapter four: focus on the controller design of the system

Chapter five: analysis the results and discussion on the result of the study

Chapter six: conclusion and recommendation of the thesis.

CHAPTER TWO

LITERATURE REVIEW AND INDUCTION MOTOR OF ELECTRIC VEHICLE

2.1 Literature review

This study describes a correlation to consider the execution of various motors in various electric automobiles with either identical or different power ratings. A thorough examination of all publications and papers has been conducted in order to discover an adequate analogy among all of the motors used in electric vehicles. A survey of many papers from prestigious journals is provided below to establish the most recent improvements in current control strategies for inverters.

2.2 Recent works

M.Tech (2015) demonstrated a Fuzzy Logic Controller for improving switching between an IC Engine and an Electric Motor [1]. The controller was designed based on the actual driving speed, planned torque, and speed-changing circumstance. A multilevel cascaded inverter for usage in electric vehicles has been proposed by L.M.Tolbe et al (2009). It simplifies EVS and allows open wiring for the majority of an electric vehicle's power system [2].

F. Roemer et al. (2019) suggested a method for simulating various CHB inverter topologies for electric vehicles with various parameters in order to choose the configuration with the greatest cost savings [3]. For this, a thorough model of the required components is used, with a focus on MOSFET switches and associated losses.

Based on past MMC research, D. Wang et al. (2019) proposed an upgraded control technique for EV applications by introducing a second-order component into the circulating current to minimize specific orders of battery current harmonics and extend battery life without increasing hardware cost [4]. The source of power Due to individual battery current limitations, In order to provide these current demands, several batteries are linked in parallel. Battery terminal voltage variations can cause circulating current to flow between parallel-connected batteries, potentially shortening their lifespan[6].

K. Abdelfatah et al. (2014). Discussed an H-Bridge power converter for an electric car's three-phase PM synchronous motor (EV). In an EV application, an H-bridge inverter feeding a 3-phase Permanent Magnet Synchronous Machine uses a synthesis of Space Vector PWM control techniques. For several reasons, such as power conditioning, power management, and fuel efficiency, power converters are becoming more prevalent in automobile applications [7].

A three-phase modified H-bridge-based multilevel inverter (MLI) architecture for driving an open-end winding induction motor was discussed by K. N. Reddy and S. Pradabane (2019). (OEWIMD). In cases including open-circuit and short-circuit switch faults, the proposed topology's functionality is investigated. An OEWIMD is fed by three single-phase modified H-bridge inverters coupled in a star configuration in the suggested MLI system [11].

Electrified automobiles (EVs), both as hybrid electric vehicles (HEVs) and as pure battery electric vehicles, are gaining headway in the personal vehicle sector, according to O.Joseffson (2015). (BEVs). A major challenge for automakers is to create a PEV with the highest drive train efficiency possible for a given battery size [13]. An aerodynamic vehicle that nonetheless appeals to customers in terms of design and storage capacity requires a lot of development time and money.

According to M. Ahsal et al. (2016), a non-linear hybrid electric vehicle (HEV) can accelerate faster by adjusting the throttle position [14]. Several recommended controllers include the proportional-integral-derivative (PID), pole placement controller, linear quadratic regulator (LQR), and state observer-based controller (OBC). An internal combustion engine, batteries for energy storage, and an electric motor for drive make up the essential parts of an updated hybrid electric vehicle..

I.T Salsabil (2016). The Pulse Width Modulation (PWM) technique is presently utilized by the majority of inverters on the market. It proposed a single-phase symmetrical hybrid sinusoidal pulse width. Inverters based on PWM technology are superior in many ways to other inverters made using conventional techniques. Inverters based on PWM frequently use MOSFETs in the output switching step [19].

2.3 Summary of literature

I look at a number of bits of information from various sources and extract important information from them. The electric vehicle system in the international automotive industry has been the subject of numerous studies and papers. However, the circulating current within the battery circuit will increase if a sizable number of batteries are connected in parallel in a power converter for an electric vehicle. The proposed solution to this issue is a novel H-bridge inverter fed induction motor (IM) drive. Additionally designed for inverter switching, pulse width modulation (PWM) is examined for common voltage/for the balanced voltage of each phase. To further optimize the battery pack and for a constant voltage, I researched the design of three single-phase H-bridge inverters with a PI controller to increase the effectiveness of transient response and steady-state performance of the electric car over a long-range drive.

According to the literature mentioned above, PI controllers are generally recommended for a variety of control systems, particularly for single phase inverters used in linear and nonlinear systems. Therefore, the design of a new topology three single-phase H-bridge inverter for the induction motor of an electric vehicle (EV) driven PI controller is not yet proposed in the total knowledge about the literature discussed above. Therefore, I find it intriguing to research the design of the PI controller for the three single-phase H-bridge inverters of an electric vehicle (EV). The open-end winding induction motor (OEWIM) is employed in the proposed topology, and each phase of the OEWIM is fed by a separate single-phase H-Bridge inverter. This suggested paper will be compared to earlier research that used the PWM and CMV techniques for control system design. However, the main issue with PWM inverters is that they produce CMV [6], [6], which results in common-mode current in the phase windings of the stator. The common-mode current warms up the motor and increases I2R loss rather than helping to convert electro-mechanical energy.

CHAPTER THREE

SYSTEM MODELING

The secondary sources of information used in this study are earlier studies published in academic journals, eBooks, Google Scholar, and case studies from the publishing industry. Additionally, the study benefited greatly from the contributions of science-direct, research gate, and Google Books, all of which were reached through Google search results.

3.1 Mathematical Modeling of Induction Motor for Electric Vehicle

The modeling of several components, including the H-bridge inverter, electric vehicle, and induction motor for EV together to form the overall EV system, is covered in this part. The SVPWM approach is first presented because it serves as the foundation for the mathematical modeling of IMs. The variable speed IM drive with PI types of controllers that are covered in later chapters is designed using the mathematical model that is described in this work. Based on the transfer function, a controller's design can control any system parameter, such as speed, torque, flux, etc. There are several ways to get the mathematical model, including starting from first principles, system identification techniques, etc.

3.1.1 Electric Motor Vehicles

Since industrial process motor drives typically work at rated speeds while electric vehicle motor drives regularly start and stop and operate in various environments, they shouldn't be compared to those used in industrial processes. The motor drive, which consists of the electric motor being used, the converter, and the electronic controller, is one of the most crucial components of any EV propulsion system.. The motor drive chosen for EVs should be able to satisfy a few requirements in order to function well as a component of the propulsion system being employed. High power density and instantaneous power are two of the characteristics.

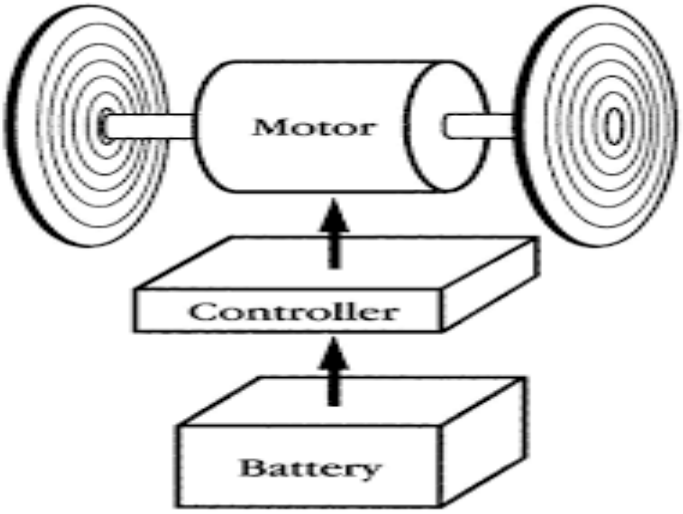


Figure 3.1 Block diagram of electric vehicle system

Since the vehicle should be able to run on any condition, the motor drive should also have a high torque while it is at low speed during starting and for climbing. Additionally, the motor drive needs to be highly efficient when employed at various speeds. The ability to provide high regenerative braking efficiency, which is crucial when working with EVs, is another vital quality that a motor drive should have [26]. An electric motor may provide a consistent torque up to its rated speed when it is operating normally. The type of motor being utilized greatly affects the power operation range in motor drives. The greatest torque is inversely proportional to speed. Different electric motors are used by manufacturers in the driving system of electric vehicles.

The Honda EV plus uses permanent magnet brushless motor and nickel-metal-hydride (NiMH) batteries, which are two technical details of a few electric vehicle types. It can travel between 80 and 100 miles on a single charge and has a top speed of roughly 80 mph. [26] General Motors' GM EVI employs an induction motor and has a range of up to 75–130 miles on NiMH batteries and up to 55–95 miles on lead acid batteries on a single charge. The majority of electric vehicles offer around the same range and speed. The cost issue is one barrier to the development of these vehicles. To improve their suitability and economic viability, battery technologies must also undergo new improvements.



Figure 3.2 Few electric vehicle models (photo courtesy Ford, Honda, Nissan, GM).

3.1.2 Challenges of Electric Vehicles

DC motors are used in the great majority of electric vehicles already on the road (4 kW and less power). The induction motor is a very well-known type of AC motor. A substantial majority of advanced power EVs employ induction motors (more than 5kW). It is common practice to manage torque and acceleration using a vector drive. The main use of BLDC motors is for low-power EVs. The battery is the primary source of energy storage in an EV. Recent advancements in in-battery technology have been credited to enormous efforts, such as the utilization of Li-particles by the next generation of EV. Before selecting a motor for an electric vehicle, it is crucial to compare them using a few key factors because different motor types exhibit different characteristics. Key attributes for electric motors used in electric cars are a straightforward design, high energy production, low maintenance requirements, and excellent control. The motor types that electric vehicle manufacturers utilize most frequently are DC motors, Induction motors, Synchronous motors, Switched Reluctance motors, and Permanent Magnet Brushless Motors.

3.1.3 Induction Motor modeling for EV

A motor is necessary for the vehicle's electric propulsion system; in this case, it is an induction motor (IM). Three-phase circuits can be more easily analyzed using a mathematical transformation known as the direct-quadrature (d-q) transformation. In balanced three-phase circuits, the three AC quantities are reduced to just two quantities through the use of the d-q transformation.

Providing sufficient torque at zero speed to enable high-speed cruising (field weakening) and conserving battery energy with the potential to operate at somewhat changeable DC battery voltage levels are the fundamental needs of electric cars [31]. Three-phase induction motors are frequently used in electric vehicles due to their high level of efficiency, superb speed control, and lack of a commutator. The revolving magnetic field is produced by the stator winding in conjunction with the three-phase AC supply. The ideal use for an AC induction motor drive is in an electric vehicle. They are generally renowned for being the commutator less compose these days. The most popular electrical drive is an induction motor or an asynchronous drive. A comprehensive examination of the electrical machinery drive system is presented in [19]. Independent control of flux and torque from separately stimulated DC drives is easier to manage. Induction motors have been employed in several applications for more than a century due to their dependability, effectiveness, and simplicity. [19] Has demonstrated the analysis and creation of an induction motor simulation model using the MATLAB / SIMULINK tools.

The (abc -dq) transformation was used to construct the model, and it can either be in the stator or rotor, depending on the application, to convert the three-phase currents into 2 axis (dq) current. Phase winding variables for stator have a relationship to abc (abc to d-q).

$$\begin{pmatrix} ids \\ iqs \end{pmatrix} = \sqrt{\frac{2}{3}} \begin{bmatrix} \cos(\theta_e) & \cos(\theta_e - \frac{2}{3}) & \cos(\theta_e - \frac{4\pi}{3}) \\ -\sin(\theta_e) & -\sin(\theta_e - \frac{2}{3}) & \cos(\theta_e - \frac{4\pi}{3}) \end{bmatrix} \begin{pmatrix} ia(t) \\ ib(t) \\ ic(t) \end{pmatrix} \quad (3.1)$$

Therefore this equation will be

$$\sqrt{\frac{2}{3}}(\cos(\theta_e)ia + \cos(\theta_e - 2.094395)ib + \cos(\theta_e - 4.18879)ic) \quad (3.2)$$

$$\sqrt{\frac{2}{3}}(-\sin(\theta_e)ia - \sin(\theta_e - 2.094395)ib - \sin(\theta_e - 4.18879)ic) \quad (3.3)$$

d-q to abc transformation blocks

The following four equations show that the transformation 2 axes into 3phase

The most effective drive techniques for the stator windings must be used, and this requires accurate modeling of each induction machine. The engineer is better able to choose the most appropriate mathematical coordinate system transformations thanks to mathematical modeling.

$$\begin{pmatrix} ia(t) \\ ib(t) \\ ic(t) \end{pmatrix} = \sqrt{\frac{2}{3}} \begin{bmatrix} \cos(\theta_e) & -\sin(\theta_e) \\ \cos(\theta_e + \frac{4\pi}{3}) & -\sin(\theta da + \frac{4\pi}{3}) \\ \cos(\theta_e + \frac{2\pi}{3}) & \cos(\theta_e + \frac{2\pi}{3}) \end{bmatrix} \begin{pmatrix} ids \\ iqs \end{pmatrix} \quad (3.4)$$

$$ia = \sqrt{\frac{2}{3}}(\cos(\theta_e)id - \sin(\theta_e)iq \quad (3.5)$$

$$ib = \sqrt{\frac{2}{3}}(\cos(\theta_e + 4.18879)id - \sin(\theta_e + 4.18879)iq \quad (3.6)$$

$$ic = \sqrt{\frac{2}{3}}(\cos(\theta_e + 2.094395)id - \sin(\theta_e + 2.094395)iq \quad (3.7)$$

This section also lists the options for coordinating transformations. MATLAB/SIMULINK was used to simulate the model that was built using the equations. A three-phase source is used with a traditional induction motor model, and the following equations or three-phase voltages are delivered to the motor (1)

$$\mathrm{V}_{as} = \mathrm{v}_m \ \mathrm{Sin}\ (w_e t) \quad (3.8)$$

$$\mathrm{v}_{bs} = \mathrm{v}_m \sin \left(w_e t - \frac{2\pi}{3}\right) \quad (3.9)$$

$$\mathrm{v}_{cs} = \mathrm{v}_m \sin \left(w_e t + \frac{2\pi}{3}\right) \quad (3.10)$$

Where w_e is the supply frequency and v_m is the terminal voltage amplitude. The three phases to two axis conversions are required to create a dynamic model of an induction motor.

These three-phase voltages are transferred within only two phases to a reference frame that rotates synchronously (d-q axis transformation). The formulae shown below can be used to do this.

The equations(3.11 and 3.12) convert three-phase stationary reference frame variables (v_{as}, $\mathrm{v}_{bs}\ and\ \mathrm{v}_{cs}$) Into two-phase stationary reference frame variables ($v_{qs}^{s}\ and\ v_{ds}^{s}$).

$$v_{qs}^{s} = v_{as} \quad (3.11)$$

$$\begin{pmatrix} v\alpha \\ v\beta \\ vo \end{pmatrix} = \frac{2}{3}\begin{bmatrix} 1 & -\frac{1}{2} & -\frac{1}{2} \\ 0 & -\frac{\sqrt{3}}{2} & \frac{\sqrt{3}}{2} \\ \frac{1}{2} & \frac{1}{2} & \frac{1}{2} \end{bmatrix}\begin{pmatrix} va \\ vb \\ vc \end{pmatrix} \tag{3.12}$$

Then, the direct and quadrature axes voltages are:

$$\begin{pmatrix} vd \\ vq \\ vo \end{pmatrix} = \frac{2}{3}\begin{bmatrix} 1 & -\frac{1}{2} & -\frac{1}{2} \\ 0 & -\frac{\sqrt{3}}{2} & \frac{\sqrt{3}}{2} \\ \frac{1}{2} & \frac{1}{2} & \frac{1}{2} \end{bmatrix}\begin{pmatrix} v\alpha \\ v\beta \\ vo \end{pmatrix} \tag{3.13}$$

Then the two-phase stationary reference frame variables $(v_{qs}^{s} \; and \; v_{ds}^{s})$ are transformed into two-phase synchronously rotating frame variables (v_{qs} and v_{ds}).

This is achieved by following equations

$$v_{qs} = v_{qs}^{s} cos\theta_e - v_{ds}^{s} sin\theta_e \tag{3.14}$$

$$v_{ds} = v_{qs}^{s} sin\theta_e + v_{ds}^{s} cos\theta_e \tag{3.15}$$

Where e= ωe t is the angle between the rotating frame and a stationary frame, and ωe is the synchronous speed at which the rotating frame rotates.

Let's now represent the variables of the stator and rotor circuits (d^s-q^s and d^r-q^r) in a frame that rotates synchronously, the d^e-q^e frame. Equation (3.16 and 3.17) are the stator circuit equations:

$$V_{qs}^{s} = R_s i_{qs}^{s} + \frac{d\Psi \mathrm{qs}^{s}}{dt} \tag{3.16}$$

$$V_{ds}^{s} = R_s i_{qs}^{s} + \frac{d\Psi \mathrm{ds}^{s}}{dt} \tag{3.17}$$

Where Ψqs^s and Ψds^s are stator flux linkages of q-axis and d-axis respectively. After converting above equations to synchronously rotating d^e-q^e frame, we get the following equations.

$$V_{qs} = R_s i_{qs} + \frac{d\Psi_{qs}}{dt} + \omega_e \Psi_{ds} \tag{3.18}$$

$$V_{ds} = R_s i_{ds} + \frac{d\Psi_{ds}}{dt} + \omega_e \Psi_{qs} \tag{3.19}$$

The rotor circuit equations are given by:

$$V_{qr} = R_r i_{qr} + \frac{d\Psi_{qr}}{dt} + \omega_e \Psi_{dr} \tag{3.20}$$

$$V_{dr} = R_r i_{dr} + \frac{d\Psi_{dr}}{dt} + \omega_e \Psi_{qr} \tag{3.21}$$

At a speed of ω_r, the rotor rotates. The d-q axes fixed to the rotor thus move relative to the synchronously rotating frame at a speed of $(\omega_e - \omega_r)$ .Thus, the actual rotor equations in the d^e-q^e frame are as follows.

$$V_{qr} = R_r i_{qr} + \frac{d\Psi_{qr}}{dt} + (\omega_e - \omega_r)\, \Psi_{dr} \tag{3.22}$$

$$V_{dr} = R_r i_{dr} + \frac{d\Psi_{dr}}{dt} + (\omega_e - \omega_r)\, \Psi_{qr} \tag{3.23}$$

As was previously stated, a state-space model of an induction motor is built in this study. As a result, defining flux linkage variables is necessary, and they are as follows:

$$F_{qs} = \omega_b\, \Psi_{qs} \tag{3.24}$$

$$F_{qr} = \omega_b\, \Psi_{qr} \tag{3.25}$$

$$F_{ds} = \omega_b\, \Psi_{ds} \tag{3.26}$$

$$F_{dr} = \omega_b\, \Psi_{dr} \tag{3.27}$$

Where ω_b is the machine's base frequency. The following equations are obtained by substituting the equations (3.24) to (3.27) in the stator and rotor equations (3.16), (3.17), (3.20) and (3.21), assuming $V_{qr} = V_{dr} = 0$

$$V_{qs} = R_s i_{qs} + \frac{1}{\omega_b}\frac{dF_{qs}}{dt} + \frac{\omega_e}{\omega_b} F_{ds} \tag{3.28}$$

$$V_{ds} = R_s i_{ds} + \frac{1}{\omega_b}\frac{dF_{ds}}{dt} - \frac{\omega_e}{\omega_b} F_{qs} \tag{3.29}$$

$$0 = R_r i_{qr} + \frac{1}{\omega_b}\frac{dF_{qr}}{dt} + \frac{(\omega_e - \omega_r)}{\omega_b} F_{dr} \tag{3.30}$$

$$0 = R_r i_{dr} + \frac{1}{\omega_b}\frac{dF_{dr}}{dt} - \frac{(\omega_e - \omega_r)}{\omega_b} F_{qr} \tag{3.31}$$

Similar to equations (3.32-3.37), the flux linkage expressions in terms of currents can be written. (3.33)–(3.38). Using equations (3.32)–(3.38) in equations (3.19)–(3.23), the electrical transient model of the IM in terms of *v* and *i* is given in matrix form as in Equation (3.26); in the inverse form, the *i*–*v* matrix could be written as in Equation (3.27). Consequently, the following is a possible way to express flux linkage expressions in terms of currents..

$$\Psi_{qs} = L_{ls} i_{qs} + L_m\left(i_{qs} + i_{qr}\right) \tag{3.32}$$

$$\Psi_{qr} = L_{lr} i_{qr} + L_m\left(i_{qs} + i_{qr}\right) \tag{3.33}$$

$$\Psi_{qm} = L_m\left(i_{qs} + i_{qr}\right) \tag{3.34}$$

$$\Psi_{ds} = L_{ls} i_{ds} + L_m(i_{ds} + i_{dr}) \tag{3.35}$$

$$\Psi_{dr} = L_{lr} i_{dr} + L_m(i_{ds} + i_{dr}) \tag{3.36}$$

$$\Psi_{ds} = L_m(i_{ds} + i_{dr}) \tag{3.37}$$

$$\begin{pmatrix} vqs \\ vds \\ vqr \\ vdr \end{pmatrix} = \begin{bmatrix} R_s + s.L_s & -\omega_e.L_s & s.L_m & -\omega_e.L_m \\ -\omega_e.L_s & R_s + s.L_s & -\omega_e.L_m & s.L_m \\ s.L_m & (\omega_e - \omega_r).L_r & R_r + s.L_r & (\omega_e - \omega_r).L_r \\ s.L_m & (\omega_e - \omega_r).L_r & R_r + s.L_r & (\omega_e - \omega_r).L_r \end{bmatrix} \begin{bmatrix} iqs \\ ids \\ iqr \\ idr \end{bmatrix} \tag{3.38}$$

$$\begin{bmatrix} iqs \\ ids \\ iqr \\ idr \end{bmatrix} = \begin{bmatrix} R_s + s.L_s & -\omega_e.L_s & s.L_m & -\omega_e.L_m \\ -\omega_e.L_s & R_s + s.L_s & -\omega_e.L_m & s.L_m \\ s.L_m & (\omega_e - \omega_r).L_r & R_r + s.L_r & (\omega_e - \omega_r).L_r \\ s.L_m & (\omega_e - \omega_r).L_r & R_r + s.L_r & (\omega_e - \omega_r).L_r \end{bmatrix}^{-1} \begin{pmatrix} vqs \\ vds \\ vqr \\ vdr \end{pmatrix} \quad (3.39)$$

The Laplacian operator is where Vqr = Vds = 0applies to a single phase IM, like the cage motor. A fourth-order linear system can be used to calculate the electrical dynamics of the IM if the speed ωr is assumed to be constant (i.e., there is infinite inertia load). Then, the currents iqs, ids, iqr, and idr can be solved from Equation by deriving the inputs vq, vds, and ωe (3.39). Equations (3.34) to (3.40) can be multiplied by ω_b to get the flow linkage expressions, which can be represented as follows on both sides.

$$F_{qs} = \omega_b \Psi_{qs} = X_{ls} i_{qs} + X_m (i_{qs} + i_{qr}) \quad (3.40)$$

$$F_{qr} = \omega_b \Psi_{qr} = X_{lr} i_{qr} + X_m (i_{qs} + i_{qr}) \quad (3.41)$$

$$F_{qm} = \omega_b \Psi_{qm} = X_m (i_{qs} + i_{qr}) \quad (3.42)$$

$$F_{ds} = \omega_b \Psi_{ds} = X_{ls} i_{ds} + X_m (i_{ds} + i_{dr}) \quad (3.43)$$

$$F_{dr} = \omega_b \Psi_{dr} = X_{lr} i_{dr} + X_m (i_{ds} + i_{dr}) \quad (3.44)$$

$$F_{dm} = \omega_b \Psi_{dm} = X_m (i_{ds} + i_{dr}) \quad (3.45)$$

Where:

$X_{ls} = \omega_b L_{ls} =$ stator leakage reactance

$X_{lr} = \omega_b L_{lr} =$ rotor leakage reactance

$X_m = \omega_b L_m =$ magnetizing reactance

Equations (3.40), (3.41), (3.43) and (3.44) are written as,

$$F_{qs} = X_{ls} i_{qs} + F_{qm} \quad (3.46)$$

$$F_{qr} = X_{lr} i_{qr} + F_{qm} \quad (3.47)$$

$$F_{ds} = X_{ls} i_{ds} + F_{dm} \quad (3.48)$$

$$F_{dr} = X_{lr} i_{dr} + F_{dm} \quad (3.49)$$

In terms of flux linkages, the stator and rotor currents can now be expressed as follows.

$$iqs = \frac{1}{Xls}(Fqs - Fqm) \tag{3.50}$$

$$iqr = \frac{1}{Xlr}(Fqr - Fqm) \tag{3.51}$$

$$ids = \frac{1}{xls}(Fds - Fdm) \tag{3.52}$$

$$idr = \frac{1}{xlr}(Fdr - Fdm) \tag{3.53}$$

Using equations (3.50) to (3.53) in equations (3.46) to (3.49), Fqm and Fdm are written as

$$F_{qm} = X_m(\frac{F_{qs} - F_{qm}}{X_{ls}} + \frac{F_{qr} - F_{qm}}{X_{lr}}) \tag{3.54}$$

$$F_{qm} = \frac{X_{m1}}{X_{ls}}F_{qs} + \frac{X_{m1}}{X_{lr}}F_{qr} \tag{3.55}$$

Also,

$$F_{dm} = \frac{X_{m1}}{X_{ls}}F_{ds} + \frac{X_{m1}}{X_{lr}}F_{dr} \tag{3.56}$$

Where, $X_{m1} = \frac{X_{m1}X_{ls}X_{lr}}{X_{ls}X_{lr}+X_{lr}X_m+X_{ls}X_m}$

After substituting equations (3.50) to (3.53) in equations (3.28) to (3.31) the stator and rotor voltage equations may then be expressed as follows.

$$V_{qs} = \frac{R_s}{X_{ls}}(F_{qs} - F_{qm}) + \frac{1}{\omega_b}\frac{dF_{qs}}{dt} + \frac{\omega_e}{\omega_b}F_{ds} \tag{3.57}$$

$$V_{ds} = \frac{R_s}{X_{ls}}(F_{ds} - F_{dm}) + \frac{1}{\omega_b}\frac{dF_{ds}}{dt} - \frac{\omega_e}{\omega_b}F_{qs} \tag{3.58}$$

$$0 = \frac{R_r}{X_{lr}}(F_{qr} - F_{qm}) + \frac{1}{\omega_b}\frac{dF_{qr}}{dt} + \frac{(\omega_e - \omega_r)}{\omega_b}F_{dr} \tag{3.59}$$

$$0 = \frac{R_r}{X_{lr}}(F_{dr} - F_{dm}) + \frac{1}{\omega_b}\frac{dF_{dr}}{dt} - \frac{(\omega_e - \omega_r)}{\omega_b}F_{qr} \tag{3.60}$$

The aforementioned equations (3.57-3.60) can now be changed to express the stator flux ($F_{qs}\ stator$): as follows in state space form:

$$\frac{dF_{qs}}{dt} = \omega b \left[v_{qs} - \frac{\omega_e}{\omega_e} F_{ds} + \frac{R_s}{x_{ls}} \{ \frac{F_{qr} X_m}{X_{lr}} + F_{qs} \left(\frac{X_m}{x_{ls}} - 1 \right) \} \right] \quad (3.61)$$

For stator flux ($F_{ds}\ stator$):

$$\frac{dF_{ds}}{dt} = \omega b \left[v_{ds} + \frac{\omega_e}{\omega_e} F_{qs} + \frac{R_s}{x_{ls}} \{ \frac{F_{dr} X_m}{X_{lr}} + F_{ds} \left(\frac{X_m}{x_{ls}} - 1 \right) \} \right] \quad (3.62)$$

For rotor flux ($F_{qr}\ rotor$):

$$\frac{dF_{qr}}{dt} = \omega b \left[(\frac{\omega_e - \omega_r}{-\omega b}) F_{dr} + \frac{R_r}{x_{lr}} \{ \frac{F_{qs} X_m}{X_{ls}} + F_{qr} \left(\frac{X_m}{x_{lr}} - 1 \right) \} \right] \quad (3.63)$$

For rotor flux ($F_{dr}\ rotor$):

$$\frac{dF_{dr}}{dt} = \omega b \left[(\frac{\omega_e - \omega_r}{-\omega b}) F_{qr} + \frac{R_r}{x_{lr}} \{ \frac{F_{ds} X_m}{X_{ls}} + F_{dr} \left(\frac{X_m}{x_{lr}} - 1 \right) \} \right] \quad (3.64)$$

3.1.4 Three-phase asynchronous machine

The induction motor is modeled by the asynchronous machine block. modeling the three-phase asynchronous machine's dynamics, also referred to as the induction machine.

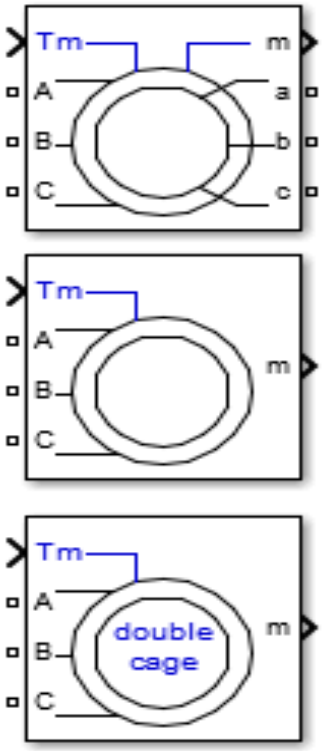


Figure 3.3 Fundamental Blocks/Machines

It is possible to create a three-phase asynchronous machine using the Asynchronous Machine block (wound rotor, single squirrel-cage, or double squirrel-cage). It is competent when used as a motor or generator. Depending on the mechanical torque's sign, a device can operate in one of several modes. Depending on whether Tm is positive or negative, the machine either functions as a motor or a generator.

They are shown by a second-order system for the mechanical part of the machine and a fourth-order state-space model for the electrical part of the machine. The stator, the source of all electrical variables and parameters, is indicated by the prime signs in the machine equations below. The arbitrary two-axis reference frame is applied to the stator and rotor in their entirety (dq frame).

3.1.5 Electrical System of the Wound-Rotor or Squirrel-Cage Machine

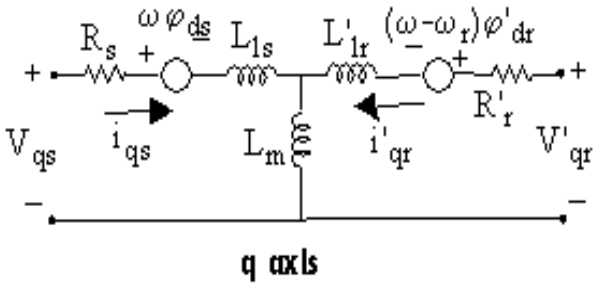


Figure 3.4 q axis of asynchronous machine

$$Vqs = Rsiqs + d\varphi qs/dt + \omega\varphi ds \tag{3.65}$$

$$Vds = Rsids + d\varphi ds/dt - \omega\varphi qs \tag{3.66}$$

$$V'qr = R'ri'qr + d\varphi'qr/dt + (\omega - \omega r)\varphi'dr \tag{3.67}$$

$$V'dr = R'ri'dr + d\varphi'dr/dt - (\omega - \omega r)\varphi'qr \tag{3.68}$$

$$Te = 1.5p(\varphi dsiqs - \varphi qsids) \tag{3.69}$$

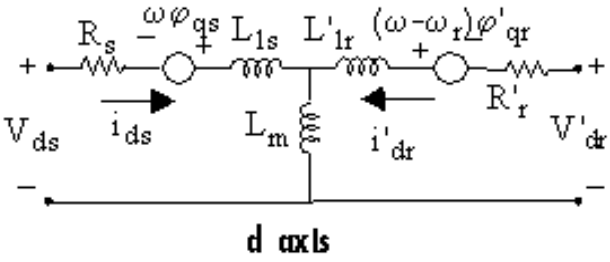


Figure 3.5 d axis of asynchronous machine

ω — *R*eference frame angular velocity

ω_r — Electrical angular velocity

$$\varphi qs = Lsiqs + Lmi'qr \tag{3.70}$$

$$\varphi ds = Lsids + Lmi'dr \quad (3.71)$$

$$\varphi'qr = L'ri'qr + Lmiqs \quad (3.72)$$

$$\varphi'dr = L'ri'dr + Lmids \quad (3.73)$$

$$Ls = Lls + Lm \quad (3.74)$$

$$L'r = L'lr + Lm \quad (3.75)$$

3.2 Power Converter/Inverter System Design

A device that transforms a DC input voltage into an AC output voltage with variable magnitude and frequency is an inverter, often referred to as a DC-AC converter [20]. According to the block diagram, the three single-phase inverters that feed the induction motor come after the power converter DC-primary AC's source, which is an external DC power source (batteries). For each phase, inverters 1, 2, and 3 are created, and the proposed controller PI controls them all. An H-bridge DC-AC module is used in the three single-phase inverters that are being developed. It has an H-bridge inverter with two internal diode-equipped MOSFETs. Before being provided to the inverter, power rectified by the converter is stored in the DC [20]. Specific inverter technology advancements are being made for use in electric vehicle applications. The inverter also extracts energy from the motor, which is now functioning as a generator in vehicles with regenerative braking, and stores it in the batteries. Three single-phase inverters (DC-adjustable AC) with variable voltage are included in the power electronics converter. Six power switches make up the inverter, and depending on the drive power limit and inverter switching frequency, they may be (IGBT).

Electric motor Both AC and DC power sources can be used to power variable speed drives. The converter consists of two components. The first component, simply known as a converter, changes an AC supply into a DC supply. A simple diode or rectifier bridge can be built or controlled switching devices like transistors can be used to provide variable DC output voltage from the converter. The second component, referred to as the inverter, converts the DC voltage source into an AC source with variable or constant voltage magnitude and adjustable frequency. One crucial factor in the performance of the drive is the caliber of the reproduced variable AC

source. Only the inverter component is required in the DC or battery-based drives to transform the DC source into a variable AC source, as indicated in the figures below.

3.2.1 Applications of Inverters

Power electronic component development has accelerated recently. Inverters are a relatively common type of power electronic component. In many industries, today, including industrial systems, power transmission, residential, and portable consumer goods, inverter systems have developed into one of the most popular power electronic systems. A device used to convert DC input voltage into AC output voltage with variable magnitude and frequency is an inverter, also known as a DC-AC converter. Many different power applications require inverters. An inverter's job is to convert DC power to AC. Voltage Source Inverters are what these are known as (VSI). Inverters are widely employed in industrial applications as well as a wide range of household applications. A battery, fuel cell, solar cell, or other DC source could serve as the input.

3.2.2 Operation of Single Phase, H-bridge Inverter

The fundamental circuit for converting DC electricity to AC is the single-phase H-bridge inverter. By turning on and off the H-bridge in the proper order, AC output voltage is produced. Depending on how switches are regulated, the bridge's output voltage, Vac, can be +Vdc, -Vdc, or 0. Because a short circuit could form across the DC source and harm the switches or the converter itself, it is important to note that both switches on one leg cannot be turned ON at the same time.

3.3 Basic power electronics control Induction Motors

The study of switching electronic components and circuits to change and regulate the flow of electrical energy is known as power electronics. The fundamental technology behind motor drives, power converters, power inverters, switching power supply, and motor soft starts is known as power electronics. By adjusting the trigger angle, inverters convert DC input into the fixed AC output; in ideal conditions, the output waveform is a perfect sine wave.

Electric motors and power electronics switching device assemblies (converters) are what make up adjustable speed electric drives [31]. ASDs are produced in a range of horsepower ratings, from 1 to more than 1000 HP. Speed and torque control, which are the induction motor's core

functions, are achieved by varying the voltage and frequency fed to the motor. The PWM method regulates the switching of the motor's supply inverter, creating a varied load at different speed settings. Voltage and frequency can be altered alone or together.

3.3.1 Power Electronics – IGBT

It is a crucial component of modern products including light ballasts, electric cars, and variable frequency motors because to its quick switching and good efficiency. Because of its rapid on/off characteristics, it can be employed in amplifiers to process complex wave patterns with pulse width modulation. By fusing the advantages of MOSFETs and BJTs, IGBTs produce high current and low saturation voltage capacity. To capture a control input, it makes use of an isolated gate built of a FET (field effect transistor).

3.3.2 Applications of IGBT

For electric motor applications, the IGBT is used in medium- to ultra-high power applications. Large IGBTs have the capacity to handle huge currents of several hundred amps and blocking voltages as high as 6kv. Inverters, converters, and other appliances that require solid state switching also employ IGBTs as its power electronic component.

3.3.3 Principle Operation of IGBT

In contrast to BJT, an IGBT only needs a minimum voltage to keep the device conducting. The IGBT can only turn ON in the forward direction because it is a unidirectional device. Accordingly, current flows from the collector to the emitter, as opposed to MOSFETs, which operate in a bidirectional way.

3.4 Modeling of H Bridge inverter Topology

3.4.1 H-Bridge Inverter Topology

A more crucial tool for obtaining an AC power signal from renewable energy sources is the DC/AC inverter (Battery or Solar panel). Based on the design of the power electronic switches, DC/AC inverters can be configured as either a half-bridge or a full-bridge topology [35]. A full bridge inverter figure is as shown:

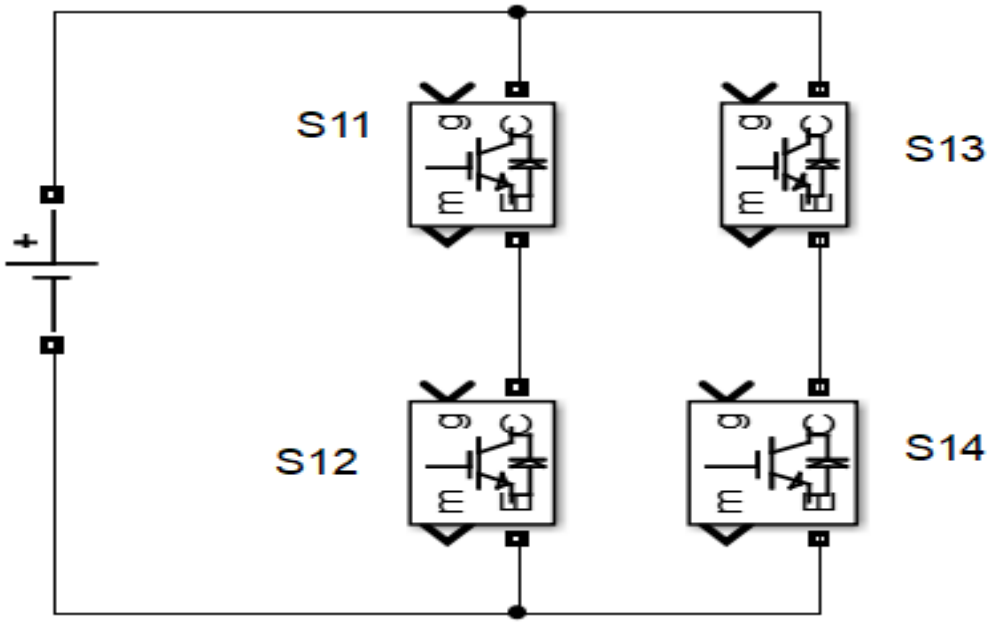


Figure 3.6 Single phase H-bridge inverter

Two legs make up a full H-bridge topology, and each branch accommodates two power semiconductor switches (MOSFET or IGBT). These legs' central support is connected across the weight [35]. Either a bipolar or a unipolar scheme can be used with the H-bridge inverter. The output voltage waveform of a bipolar inverter is between (+Vdc, -Vdc) output connections, but the output voltage signal of a unipolar system, also known as a three-level inverter, is between (+Vdc, 0, -Vdc). In contrast to similar outcomes in the case of bipolar inverter switching, the Total Harmonic Distortion of the output waveforms is optimal and minimal in the unipolar inverter design[39].

Inverter designs come in a wide variety. The so-called H-bridge topology is the most widely used [30]. An inverter's main function is to change DC electricity into AC power, as was already established. [30] Uninterruptible power supply, induction heating, high-voltage direct current power transmission, variable frequency drives, electric vehicle drives, and other renewable energy applications are a few of the technologies that depend on inverters. While each of these systems uses inverters to accomplish a different objective, they all employ a DC input to produce AC power.

An H-bridge electrical circuit modifies the polarity of a voltage applied to a load. The standard graphical representation of this type of circuit is where the term "H-bridge" originates. An H-bridge is built with four switches (solid-state or mechanical). As soon as the switches S1 and S4 (shown in the first figure) are closed, a positive voltage is provided across the motor (and S2 and S3 are open). By closing S2 and S3 switches and opening S1 and S4 switches, this voltage is switched, allowing the motor to run in the opposite direction.

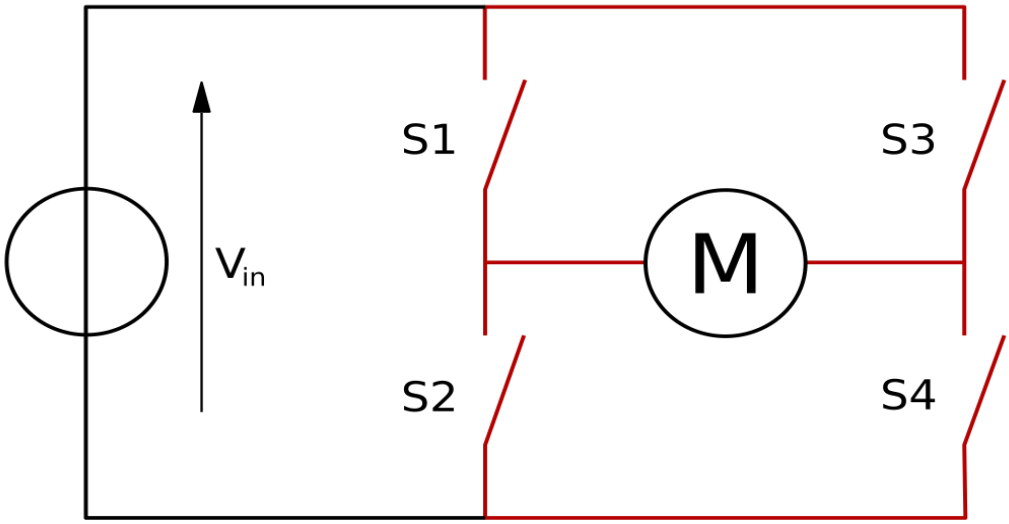


Figure 3.7 Structure of an H-bridge (highlighted in red)

The switches S1 and S2 should never be closed at the same time using the aforementioned nomenclature since doing so would result in a short circuit on the input voltage source. Both S3 and S4 switches function identically. Shoot-through is the term for this situation.

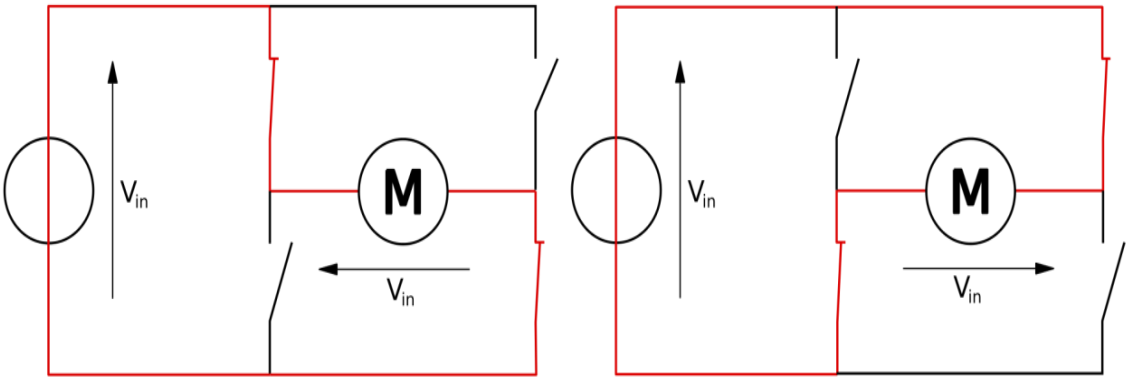


Figure 3.8 the two basic states of an H bridge

Inverters frequently employ the H-bridge. A single-phase bridge inverter is another name for the device. The H-bridge will create a square wave voltage waveform across the load when driven by a DC supply. For a completely inductive load, the inductance, switching frequency, and input voltage would all affect the peak of the current waveform.

3.4.2 Three single-phase H-Bridge Inverter

The fundamental component of a H-bridge inverter is this kind of inverter. There are four per-phase switches in it. To reduce the number of batteries linked in parallel, a new distributed inverter topology is suggested. The computation is based on the quantity and combination of batteries needed to power a 50hp, 148 V, and 50 Hz IM. The IM's input power is taken to be 37 kW. In the suggested topology, the total input power is divided among the three single-phase H-bridge inverters. So the input power per phase is 12.33 kW.

In vehicles, many batteries are connected in parallel and series to supply rating current and voltage for motors. However, as many batteries are connected in parallel there is a circulation current through the shunt batteries. In a three-phase system, the shunt batteries deliver the voltage for the motor. Therefore, the dc-link is separated for each phase to minimize the current circulation

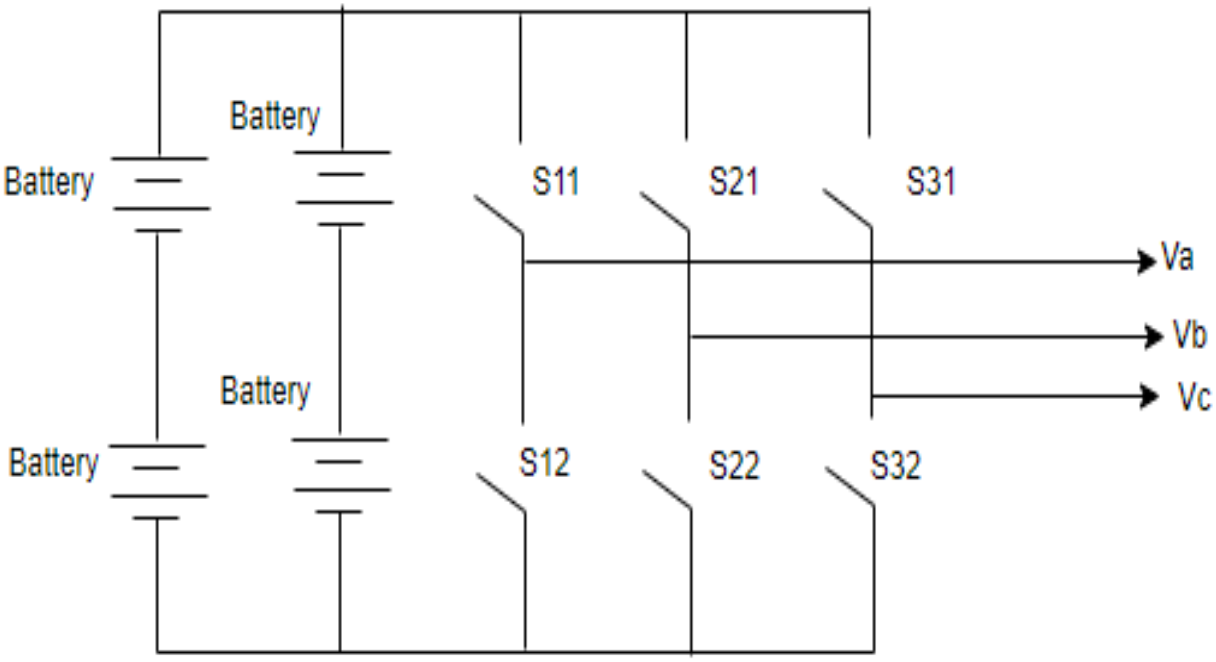


Figure 3.9 DC-AC conversion (voltage source inverter) for three phase

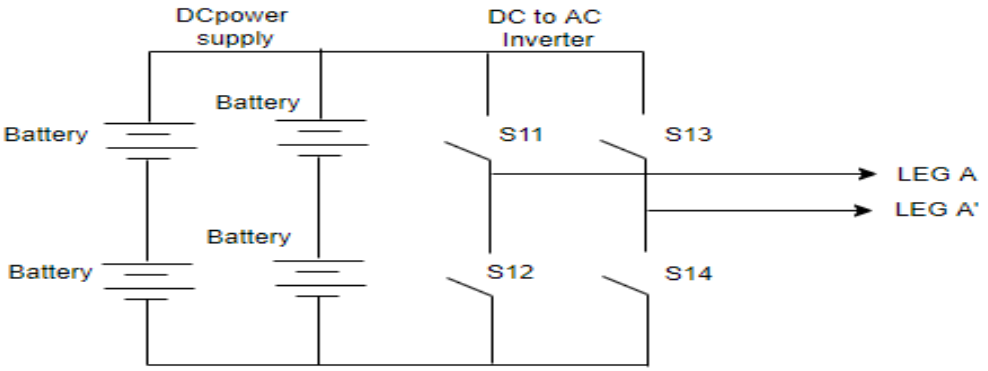


Figure 3.10 DC-AC conversion (voltage source inverter) for first phase

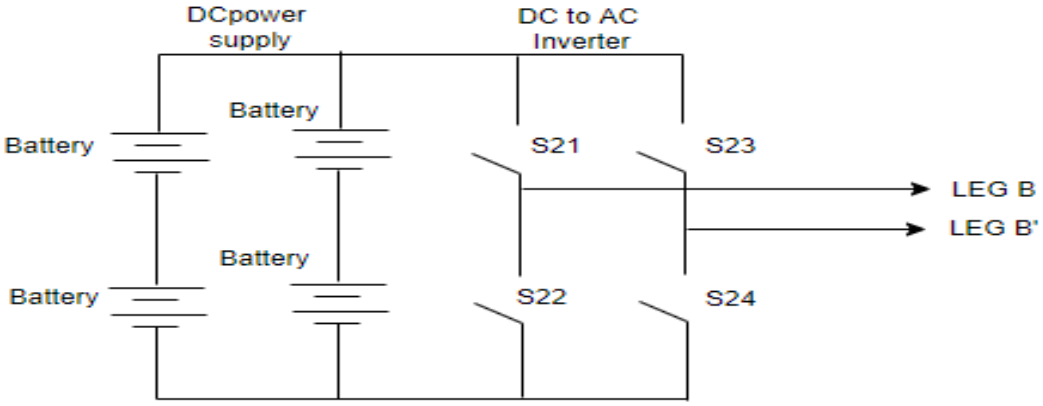


Figure 3.11 DC-AC conversion (voltage source inverter) for second phase

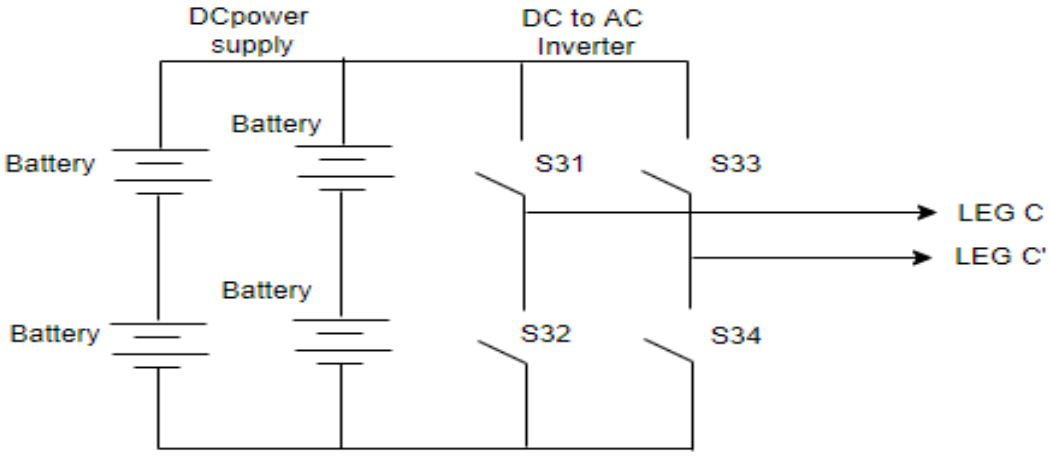


Figure 3.12 DC-AC conversion (voltage source inverter) for the third phase

Three single-phase H-Bridge inverters are utilized in this topology (namely, inverters A, B and C). Sx1, Sx2, Sx3, and Sx4 are the four discrete switches found in each single-phase H-Bridge inverter, where x is one of A, B, or C. Each phase winding of the stator is connected to a single-phase H-Bridge inverter in turn. Each inverter's dc-link voltage is Vdc. Despite having four discrete states per single-phase H-Bridge inverter, they can only output discrete voltage levels of +Vdc/2, 0 and -Vdc/2. This study provides three single-phase H-Bridge inverters fed by an OEWIM drive, which reduces the parallel battery combination.

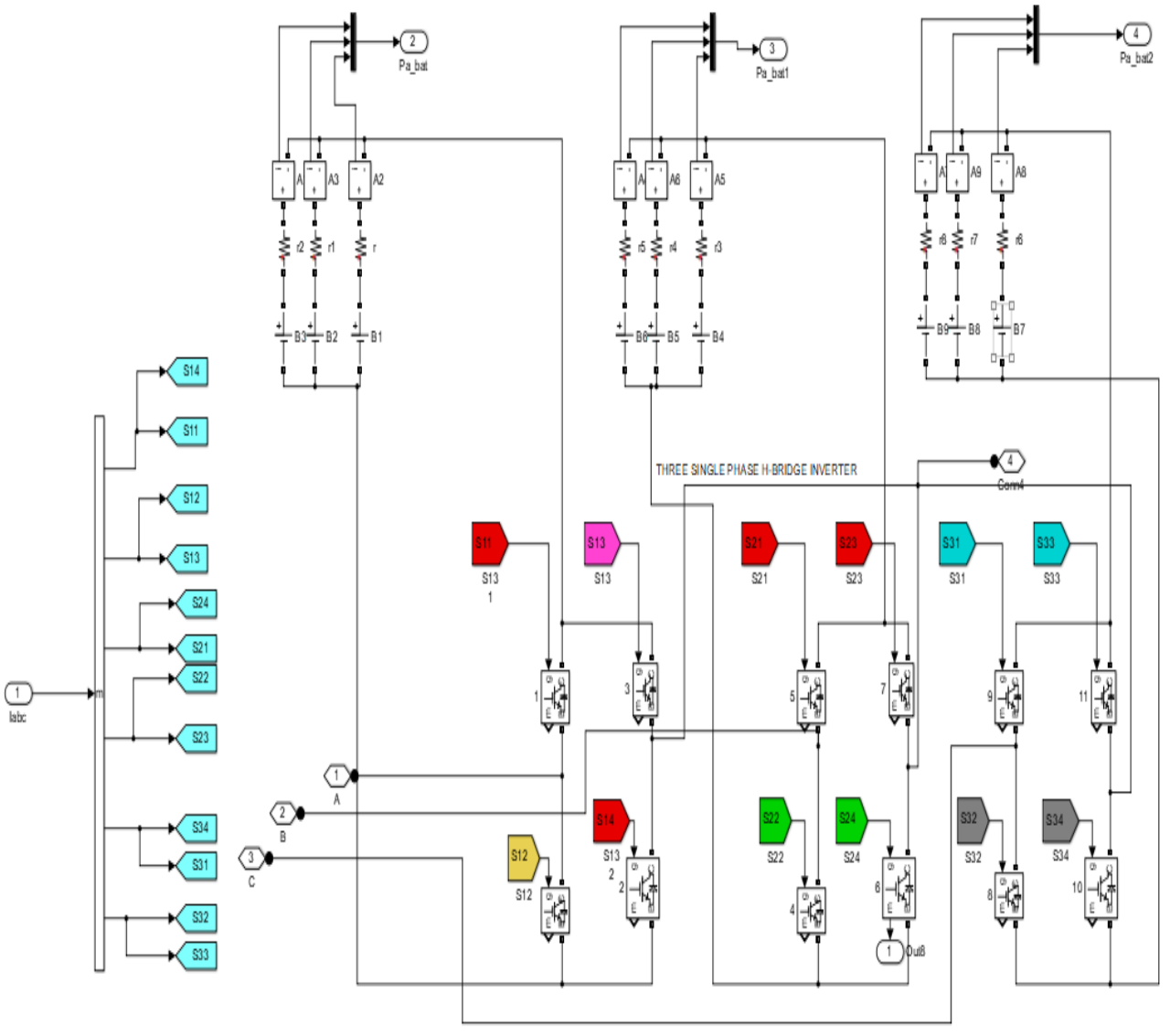


Figure 3.13 Proposed three single-phase H-Bridge inverters fed open-end winding induction motor drive

3.4.3 I/O and O/P specifications for a system of electric vehicles

The needed traction force for the vehicle, the motor power rating, the gear ratio, the range in kilometers, the battery energy rating, and the battery ampere-hour rating are among the [37] elements of the electric vehicle system that are used to determine the output parameters.

A force is making an attempt to stop the moving vehicle's momentum. The different resistance forces include aerodynamic drag, slope resistance, and tire rolling resistance.

A. Rolling Resistance -

Tire deflection, tire slippage, and air flow around the wheel are all factors that contribute to rolling resistance in vehicles. The rolling resistance force's mathematical representation is

$$F_r = f_r * M * g * cos\alpha \tag{3.76}$$

B. Aerodynamic Drag -

As a car is moving against the wind, the amount of resistance it experiences If the vehicle is moving in the direction of the wind, however, this force will assist the tractive force..

$$F_d = \frac{\rho}{2} * C_d * A_f * V^2 \tag{3.77}$$

C. Grading Resistance -

A vehicle going up a hill will experience grading resistance, which pulls the vehicle downward. But when the vehicle descends the slope, this grading resistance balance out the tractive force. The following is an expression for the grading resistance force.

$$F_g = M * g * sin\alpha \tag{3.78}$$

D. Equations governing Vehicle modeling [80]-[84]

The acceleration force is obtained by deducting the resistance forces from the tractive force.

$$F_t = F_r + F_d + F_g + F_a \tag{3.79}$$

(required total max torque force at the wheel)

The components that make up the acceleration force are the mass factor, which is the factor used to convert the rotating mass of the rotor to linear mass, the mass of the vehicle body, and the change in speed..

$$\mathrm{F_a} = \delta * \mathrm{M}\left(\frac{\mathrm{dV}}{\mathrm{dt}}\right) \tag{3.80}$$

(Acceleration Force)

The following equation determines how much torque the motor must produce to achieve the desired acceleration.

$$T_m = \frac{n * F_t * r}{G * \eta_t} \tag{3.81}$$

The equation below can be used to determine the motor's maximum power rating.

$$P_{out-mot} = n * F_t * V_{max} \tag{3.82}$$

The input power to the motor can be calculated by taking into account the normal value for efficiency and dividing the output power by it.

$$P_{in-mot} = \frac{P_{out-mot}}{\eta_m} \tag{3.83}$$

Calculating the resistance forces and multiplying them by the necessary range will yield the battery's energy rating.

$$\text{Energy (Wh)} = \text{ Force (N)} * \text{Distance (Km)} \tag{3.84}$$

Electric vehicles typically have a single gear transmission, which may be estimated using the equation below.

$$G = \frac{RPM * Tire\ circumference}{60 * Top\ speed} \tag{3.85}$$

Ah/km can be computed by dividing the Wh/km needed by the vehicle by the battery's Voltage rating.

$$\frac{(Wh/km)}{V} = \left(\frac{ah}{km}\right) \tag{3.86}$$

E. Induction motor Specifications –

The motor used in this case study has the following specifications.

Table 3.1: Specifications and parameters for induction motor

Parameters	Values
Power	50 HP (37 kW)
Voltage	148 V
Frequency	50Hz
Ras(**Main winding stator resistance**)	1.8180 ohms
Llas (**Main winding stator leakage inductance**)	$0.0067H$
Rar(**Main winding rotor resistance**)	$3.7080\ ohms$
Llar (**Motor winding rotor leakage inductance**)	$0.0050\ H$
Lms **Main winding mutual inductance**	$0.1595\ H$
Rbs **Auxiliary winding stator resistance**	$6.4260\ ohms$
Llbs **Auxiliary winding stator leakage inductance**	$0.0077\ H$
Synchronous speed (R.P.M)	3000 rpm
J (inertia)	0.0148
F (friction force)	0
Poles pairs	2

F. Indirect Field Oriented Control -

The direct axes of stator currents and the vector-based quadrature axes are the main targets of the Field Orientated Control (FOC) [37] approach. These projections make an AC machine's control more similar to a DC machine. The flux component, which is normally considered to be aligned with the d co-ordinate, and the torque component, which is often taken to be aligned with the q co-ordinate, are used in a field-oriented controlled machine. Due to its ability to operate AC motors in closed loop over a broad range of speeds, even those above the specified speed using a field weakening method, indirect field oriented control strategy is frequently utilized in this context.

G. Equations governing IFOC –

Calculated from torque reference Te* is the stator quadrature-axis current reference (iqs*).

$$I_{qs}* = \frac{2}{3} * \frac{2}{p} * \frac{Lr}{Lm} * \frac{Te*}{|\psi r|est} \tag{3.87}$$

The expected value $|\psi r|est$ for the rotor flux linkage is provided by

$$|\psi r|est = \frac{Lm * ids}{1 + \left(\frac{Lr}{Rr}\right) * s} \tag{3.88}$$

The stator direct-axis current reference ids* is calculated using the rotor flux reference input |ψr|*.

$$I_{ds}* = \frac{|\psi r|}{Lm} \tag{3.89}$$

For the purpose of transforming coordinates, the rotor flux position θe is calculated using the rotor speed ωm and the slip frequency ωsl.

$$\theta_e = \int (\omega m + \omega_{sl})\, dt \tag{3.90}$$

The motor characteristics and the quadrature axis current iqs are utilized to compute the slip frequency.

$$\omega_{sl} = \frac{Lm}{|\psi r|est} * \frac{Rr}{Lr} * iqs \tag{3.91}$$

The most effective drive techniques for the stator windings must be used, and this requires accurate modeling of each induction machine. The engineer is better able to choose the most appropriate mathematical coordinate system transformations thanks to mathematical modeling.

3.4.4 Electric motor sizing

This section will present the mathematical formula used to calculate the power and torque of an electric motor using the information from Tables 3.7 and 3.8. Calculating the applied forces to the vehicle while accounting for drag, rolling, and overall vehicle weight is necessary to calculate the power and torque. The four primary forces at work will be taken

into consideration: the rolling resistance force, the drag resistance force, the weight force on a ramp at an angle, and the dynamic force [38].

As listed here, the vehicle's four primary forces are, from (3.85) to (3.88) [38].

$$F_{roll} = m.g.c_{re} \tag{3.92}$$

$$F_{drag} = \frac{1}{2}.\rho_{air}.A_{front}.c_d.v^2 \tag{3.93}$$

$$F_{accel} = m.a \tag{3.94}$$

$$F_{ramp} = m.g.\sin\left(\theta.\frac{\pi}{180^0}\right) \tag{3.95}$$

Speed and force both contribute to potency. In this instance, it is stated by (3.89).

$$P_1 = v.\left(F_{roll} + F_{drag} + F_{accel} + F_{ramp}\right) \tag{3.96}$$

The motor's efficiency must be taken into account while calculating motor power:

$$P_{motor} = \frac{P_1}{\eta_{motor}}.100 \tag{3.97}$$

The vehicle's wheel torque comes from (3.37).

$$T_{wheel} = \left(F_{roll} + F_{drag} + F_{accel} + F_{ramp}\right).r_{wheel} \tag{3.98}$$

3.5 Electric vehicle battery rating calculation

Based on the supplied route that was researched, the following sections will demonstrate the techniques utilized to determine the battery pack and electric motor size.

3.5.1 EV design – battery calculation

One of a battery electric vehicle's (BEV) most crucial parts is the high voltage battery. Other parts and characteristics of the car are significantly impacted by the battery specifications, such as:

- ✓ maximum regeneration brake torque
- ✓ maximum traction motor torque
- ✓ vehicle total weight

- ✓ vehicle range

Almost all crucial components of a pure electric vehicle (EV) are determined by the high voltage battery's specifications.

The highest continuous electrical power that may be produced depends on the battery voltage level. Voltage U [V] and current I [A] are multiplied to produce power P [W]:

$$P = U * I \tag{3.99}$$

The high voltage wires' diameter increases with increasing current, and so do thermal losses. For this reason, a maximum current limit should be used, and a greater voltage should be used to achieve the nominal power. We're going to use 148 V as the nominal voltage for our application.

We calculated the study EV design's E_{avg} usage for propulsion Ep to be $137.8\ \mathrm{Wh/km}$ on the WLTC driving cycle. The vehicle's Eaux [Wh/km], auxiliary equipment, such as the 12 V electrical systems, heating, cooling, etc., must also be powered by the high voltage battery. Additionally, we must take into account the powertrain's effectiveness η_p *[-]* while converting electrical energy to mechanical energy.

$$E_{avg} = \left(E_p + E_{aux}\right).(2 - \eta p) \tag{3.100}$$

The average amount of electrical power used by the constant loads (heating, brake lights, wipers, etc.) and intermittent loads (headlights, multimedia, etc.) is 430 W. The WLTC cycle lasts for 1800 s (0.5 h), and it supplies the auxiliary loads with 215 Wh of energy. When we divide the average energy consumption for the auxiliary loads Eaux by the length of the WLTC driving cycle, the result is 9.241 Wh/km (23.266 km).

$$\begin{aligned} E_{au} &= 137.8 + 9.241).1.1 \\ &= 161.7451 Wh/km \end{aligned} \tag{3.101}$$

The battery pack will be created with a 161.7451 Wh/km average energy consumption into consideration.

3.5.2 Battery packs designs

Battery cells are arranged in strings and modules to create high voltage battery packs in any circumstance. A battery cell is the smallest unit of voltage.

In order to create a battery pack, battery modules can also be connected in series and/or parallel. Depending on the characteristics of the battery, there might be varying degrees of flexibility. The number of series-connected cells determines the voltage of the overall battery pack. To increase the battery's current capacity, additional strings must be linked in parallel.

3.5.3 Battery packs calculation

We'll examine a number of battery cell models on the market before deciding which battery cells our pack will contain. In this paper, we'll exclusively discuss lithium-ion batteries.

Table 3.2 the battery cells' input parameters.

Manufacturer	Panasonic	A123 − systems	Molicel	A123 − syste	Toshiba	Kokam
Type	cylindrical	Cylindrical	cylindrical	pouch	pouch	pouch
Model T	NCR18650B	ANR26650ml_B	ICR − 18650K	20Ah	5.4Ah	SLPB7570270
Mass [**kg**]	0.0485	0.076	0.05	0.496	0.51	0.317
Capacity [**Ah**]	3.2	2.5	2.6	19.5	5.4	15.6
Voltage [**V**]	3.6	3.3	3.7	3.7	7.2	3.6
C − rate (**cont.**)	1	10	1	1	1	2
C − rate (**peak**)	1	24	2	10	1	3

- The **battery cell energy** E_{bc} [Wh] is calculated as:

$$E_{bc} = C_{bc}.U_{bc} = 7.2 * 5.4 = 38.88Wh \quad (3.102)$$

where:

Cbc [Ah] – Capacity of the battery cells

Ubc [V] – Voltage of the battery cells

- Battery cell energy density is calculated using the following formula:

uV [Wh/m3] density of volumetric energy

$$u_V = \frac{E_{bc}}{V_{cc(pc)}} = \frac{38.88}{0.260590} = 149.2\text{Wh/m3} \quad (3.103)$$

density of gravimetric energy, u_G [Wh/kg]

$$u_G = \frac{E_{bc}}{m_{bc}} = \frac{38.88}{0.51} = 76.24\text{Wh/kg} \quad (3.104)$$

Where:

m_{bc} [kg] – mass of battery cell

Table 3.3 The energy density of each cell.

Manufacturer	Pana − sonic	A123 − systems	Molicel	A123 − systems	Toshiba	Kokam
Type	Cylindrical	Cylindrical	Cylindrical	Pouch	Pouch	Pouch
Model T	NCR18650B	ANR26650ml_B	ICR − 18650K	20Ah	5.4Ah	SLPB7570270
Energy [Wh]	11.52	8.25	9.62	64.35	38.88	56.16
Volume [**l**]	0.017553	0.034510	0.017716	0.26330	0.260590	0.171741
Energy density Gravimetric [**Wh/kg**]	237.53	108.55	192.40	129.74	76.24	177.16
Energy density volumetric [**Wh/l**]	656.31	239.06	543.01	244.38	149.2	327

We determine the fundamental parameters of the high voltage battery using the aforementioned cell attributes and the necessary criteria (nominal voltage, the average energy consumption, and vehicle range). To calculate the necessary battery pack total energy Ebp [Wh], the vehicle's range Dv [km] and average energy consumption Eavg [Wh/km] are multiplied. We'll build a high-voltage battery pack with a 250 km driving range for this thesis.

$$E_{bp} = E_{avg}.D_v = 161.7451 * 250 = 40436.275Wh = 40.44kWh \quad (3.105)$$

The computations that will be carried out for each cell type are as follows. For the purposes of this new thesis, we will assume that the battery pack consists of of a number of parallel strings.

$$N_{cs} = \frac{U_{bp}}{U_{bc}} = \frac{148}{7.2} = 21\ cells \quad (3.106)$$

The amount of energy in a string, E_{bs} [Wh]:

$$E_{bs} = N_{cs}.E_{bc} = 21 * 38.88 = 816.48Wh \quad (3.107)$$

The total number of strings N_{sb} [-] :

$$N_{sb} = \frac{E_{bp}}{E_{bs}} = \frac{40436}{816.48} = 50\ cells \quad (3.108)$$

Now that we know how many strings there are and how much energy each string contains, The total energy of the battery pack, Ebp [Wh], can be recalculated.

$$E_{bp} = N_{sb}.E_{bs} = 50 * 816.48 = 40.824kW \quad (3.109)$$

The battery pack capacity C_{bp} *[Ah]:*

$$C_{bp} = N_{sb}.C_{bc} = 50 * 5.4 = 270Ah \quad (3.110)$$

The total number of cells in the battery pack, N_{cb} [-]:

$$N_{cb} = N_{sb}.N_{cs} = 50 * 21 = 1050\ cells \quad (3.111)$$

We will use data from simply the battery cells in this part to calculate the volume of the battery pack. In fact, there are more aspects to take into account, such as wiring, battery housing, cooling circuits, electrical circuits, and cooling circuits.

The overall mass of the battery pack (kg)

$$m_{bp} = N_{cb}.m_{bc} = 1050 * 0.51 = 535.5kg \quad (3.112)$$

The battery pack volume (m^3)

$$V_{bp} = N_{cb}.V_{cc(pc)} = 532.44 * 0.51 = 273.1m^3 \quad (3.113)$$

The peak current of string I_{spc} [A]:

$$I_{spc} = C - rate_{bcp}.C_{bc} = 1 * 5.4 = 5.4A \quad (3.114)$$

Peak current of Battery pack (A)

$$I_{bpp} = I_{spc}.N_{sb} = 5.4 * 50 = 270A \quad (3.115)$$

The voltage U_{bp} [V] and peak current I_{bpp} [A] of a battery pack are multiplied to determine the peak power P_{bpp} [W] of the battery pack.

$$P_{bpp} = I_{bpp}.U_{bp} = 270 * 148 = 39.96kW \quad (3.116)$$

The continuous current of string (I_{scc} [A])

$$I_{scc} = C - rate_{bcc}.C_{bc} = 1 * 5.4 = 5.4A \quad (3.117)$$

The continuous current of battery pack (Ibpc [A]) :

$$I_{bpc} = I_{scc}.N_{sb} = 5.4 * 50 = 270A \quad (3.118)$$

The battery pack voltage Ubp [V] and battery pack continuous current Ibpc [A] are multiplied to get the battery pack continuous power Pbpc [W].

$$P_{bpc} = I_{bpc}.U_{bp} = 270 * 148 = 39.96kW \quad (3.119)$$

Table 3.4: The results of the equations above

$Manufacturer$	$panasoni$	$A123 - syste$	$Molicel$	$A123 - syster$	$Toshiba$	$kokam$
$\#\ of\ cells\ in\ string\ [-]$	122	122	109	122	21	112
$String\ energy\ [Wh]$	1290	1007	1049	7851	816.48	6290
$\#\ of\ strings\ [-]$	32	41	39	6	50	7
$BP\ energy\ [kWh]$	41.29	41.27	40.89	47.10	40.824	44.03
$BP\ capacity\ [Ah]$	102.4	102.5	101.4	117	270	109.2
$\#\ total\ cells\ [-]$	3584	5002	4251	732	1050	784
$BP\ mass\ [kg]\ *$	173.8	380.2	212.6	363.1	535.5	248.5
$BP\ volume\ [l]\ *$	63	173	75	193	273.1	135
$BP\ peak\ current\ [A]$	102.4	2460	202.8	1170	270	327.6

$BP\ peak\ power\ [kW]$	40.96	984	81.12	468	39.96	131.04
$BP\ continuous\ current\ [A]$	102.4	1025	101.4	117	270	218.4
$BP\ continuous\ power\ [kW]$	40.96	410	40.56	46.8	39.96	87.36

BP – battery pack,

* – choosing to focus on battery cells.

3.6 Voltage source inverter

Voltage Source Inverters (VSIs) have recently attracted greater study attention in high power applications due to a number of properties, such as their ability to provide output voltage signals of high quality while minimizing switching losses by semiconductor devices [35]. Inverters use a variety of modulation techniques to produce the required output voltage. According to switching frequency, these inverters are divided into categories [35]. The Pulse Width Modulation is a well-liked technique that operates at a high switching frequency (PWM).

The DC voltage for VSI comes from a variety of sources. A battery bank, wind energy, or solar photovoltaic cells could all be the source. Additionally, the AC voltage supply that is converted to DC after a rectifier might be considered another source of DC voltage [33]. If the amount of source voltage is independent of the load that is connected to the source, the source is said to be stiff. In VSI, the input voltage supply is regarded as stiff [8]. The power switches that determine the output shape are the six switches (S1 to S6). The lower switches and the upper switches work well together [33]. The Pulse Width Modulation is a well-liked technique that operates at a high switching frequency (PWM).

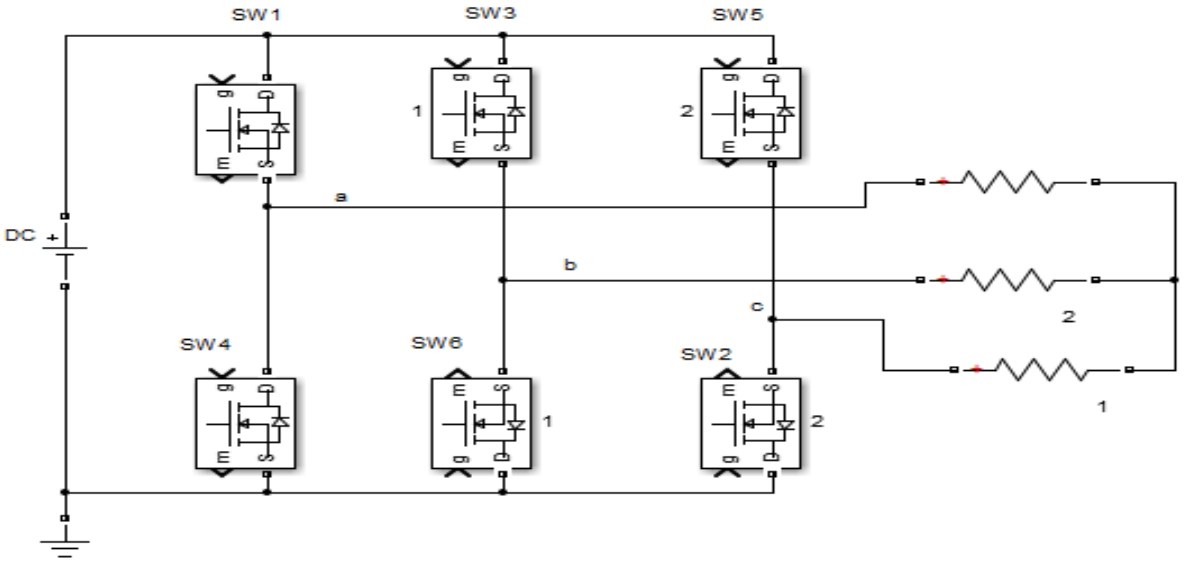


Figure 3.14 schematic diagram of two level VSI

According to Figure 3.10, eight switching status structures may be produced in the two-level VSI depicted in Table 3.9. When the status is (1), one of the top switches is conducting, and when the status is (2), the bottom switch is conducting (0). The appropriate inverter legs are identified by the three digits in the status (a, b, and c). For instance, the switching status [100] shows that one of the top switches, S1, is conducting in the leg while two lower switches, S6 & S1, are conducting in the inverter (a). The other conditions are active situations. Two statuses exist: [111] and [000], both of which result in a zero output.

Table 3.5 Switching conditions and on-status switches

Space vector		Switching conditions	On-status switch
Zero vector	V0	111	S1, S3, S5
		000	S4, S6, S2
Active vector	V1	100	S1, S6, S2
	V2	110	S1, S3, S2
	V3	010	S4, S3, S2
	V4	011	S4, S3, S5
	V5	001	S4, S6, S5
	V6	101	S1, S6, S5

Table 3.6 Switching conditions and on-status switches

Switching state			Line to Neutral			Line to Line voltage			Voltage vector
A	B	C	VAN	VBN	VCN	VAB	VBC	VCA	
0	0	0	0	0	0	0	0	0	V0=0
1	0	0	2/3vdc	-1/3vdc	-1/3vdc	Vdc	0	Vdc	$V1 = \frac{2}{3}Vdce^{j.0}$
1	1	0	1/3vdc	1/3vdc	-2/3vdc	0	Vdc	- Vdc	$V2 = \frac{2}{3}Vdce^{j.\frac{\pi}{3}}$
0	1	0	-1/3vdc	2/3vdc	-1/3vdc	- Vdc	Vdc	0	$V3 = \frac{2}{3}Vdce^{j.\frac{2\pi}{3}}$
0	1	1	-2/3vdc	1/3vdc	1/3vdc	- Vdc	0	Vdc	$V4 = \frac{2}{3}Vdce^{j.\pi}$
0	0	1	-1/3vdc	-1/3vdc	2/3vdc	0	- Vdc	Vdc	$V5 = \frac{2}{3}Vdce^{j.\frac{4\pi}{3}}$
1	0	1	1/3vdc	-2/3vdc	1/3vdc	Vdc	- Vdc	0	$V6 = \frac{2}{3}Vdce^{j.\frac{5\pi}{3}}$
1	1	1	0	0	0	0	0	0	V7=0

3.7 Pulse Width Modulation (PWM)

PWM is a technique utilized in a number of power electronics applications. SVPWM is a well-liked method for controlling AC motor drives. The sine wave modulates the triangle carrier wave, and the point of intersection determines the inverter's switching points. Power electronics, such as motor control, is where PWM is mostly used. The drawback of producing analog signals is that the PWM resolution rapidly declines with the necessary signal bandwidth. SVPWM might therefore be utilized for more sophisticated control of AC motor drives to circumvent the disadvantages of this approach.

Pulse-width modulation (PWM) is a method for reducing an electrical signal's average strength by discretizing the signal into smaller, more manageable portions. In order to control the average voltage and current given to the load, the switch between supply and load is swiftly cycled on and off. While the switch is turned on for longer than when it is off, more total power is delivered to the load. The PWM switching frequency must be high enough not to affect the load in order for the load to interpret the produced waveform as smoothly as feasible. To divide

an electrical signal into various components in order to lower the average power delivered by the signal (chopping). By switching the supply, the average voltage fed to the load is controlled. The average voltage provided to the load is managed by switching the supply. By turning on and off the various inverter switches, we may change the pulse width. The analog devices are managed via pulse width modulation.

3.7.1 Simulink model of Uni-Polar Pulse Width Modulation (PWM)

For the PWM unipolar scheme, two sinusoidal reference waveforms with the same frequency and amplitude but a 180^{o} phase shift are frequently required. The triangle signal is compared with two sinusoidal reference signals, one positive and the other negative. At the fundamental frequency, the inverter's output voltage shifts from zero to either a positive or negative value. The voltage source inverter is crucial and must adhere to the allowed range (VSI). Several methods are suggested to generate as much sinusoidal output signal as is practicable. One of these techniques is the use of an inverter with Sinusoidal Pulse Width Modulation (SPWM). Industrial inverters frequently employ SPWM. This paper presents the results of the study on the performance of a three-phase H-bridge inverter using the SPWM technology. The SPWM system is modeled using MATLAB - Simulink. This thesis examines a unipolar PWM method.

3.7.2 sinusoidal pulse width modulation

PWM is used on variable speed drives, which are a component of several modern industrial applications. When it comes to voltage source inverters, sinusoidal pulse width modulation is most frequently used (SPWM). With the help of this method, the pulse width is modified in proportion to the predicted amplitude of a reference signal at the pulse's center. When comparing a sinusoidal waveform f_r with a triangular carrier waveform f_c, switching signals are created, as can be observed after simulating a unipolar system. The reference frequency signal f_r, which regulates the modulation ratio m_a and peak amplitude, determines the inverter output frequency. The carrier frequency controls the number of pulses every half-cycle. The SPWM inverter uses a continuous DC input to produce sinusoidal form at a certain frequency. Two SPWM techniques—SPWM with unipolar switching and SPWM with bipolar switching—are available for H-bridge inverters. As described by the modulation index, m_a, the amplitude modulation ratio is

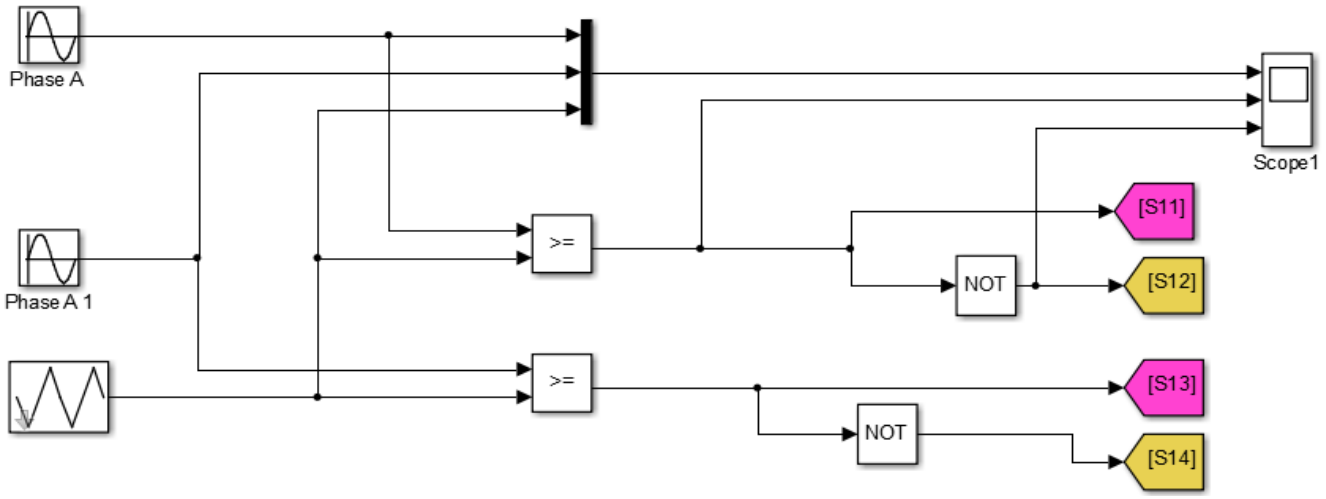


Figure 3.15 Uni-polar PWM inverter for phase A

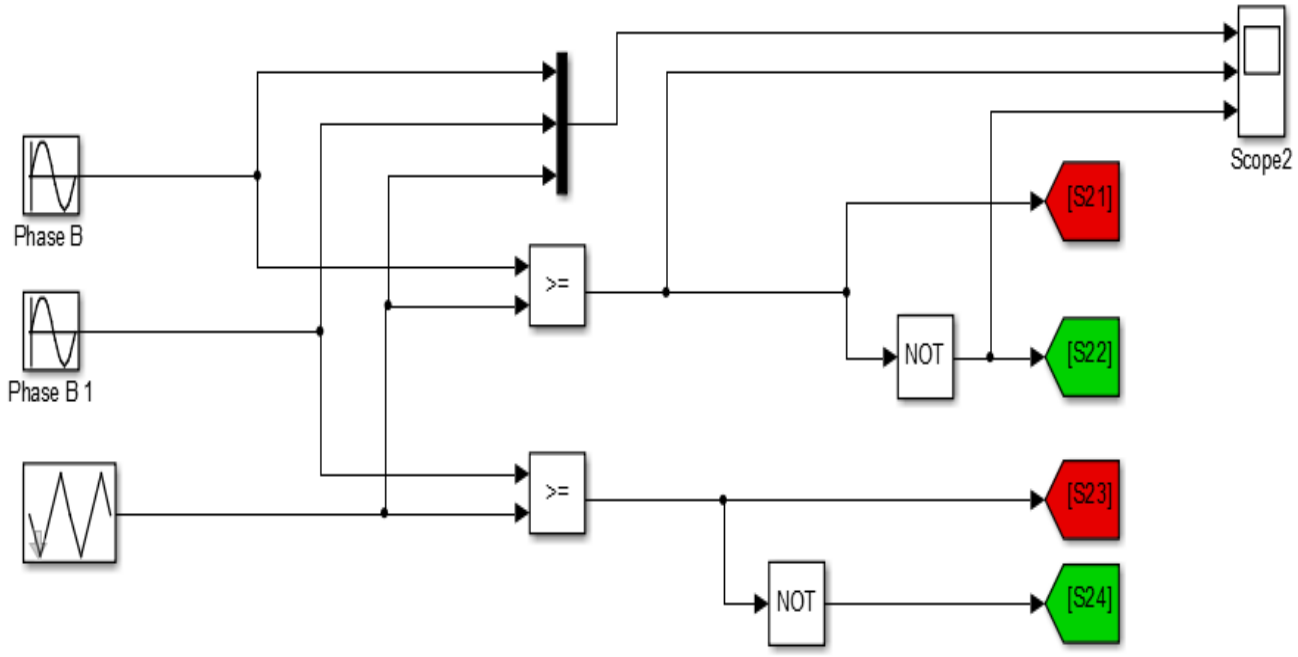


Figure 3.16 Uni-polar PWM inverter for phase B

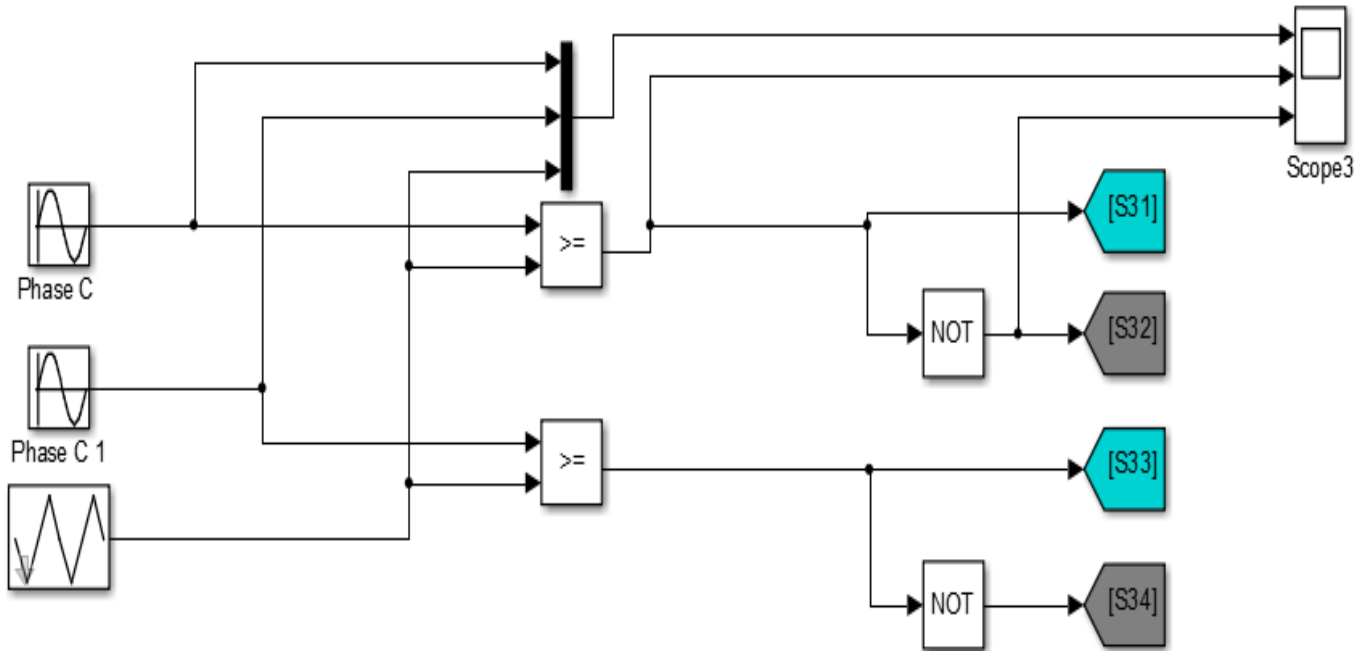


Figure 3.17 Uni-polar PWM inverter for phase C

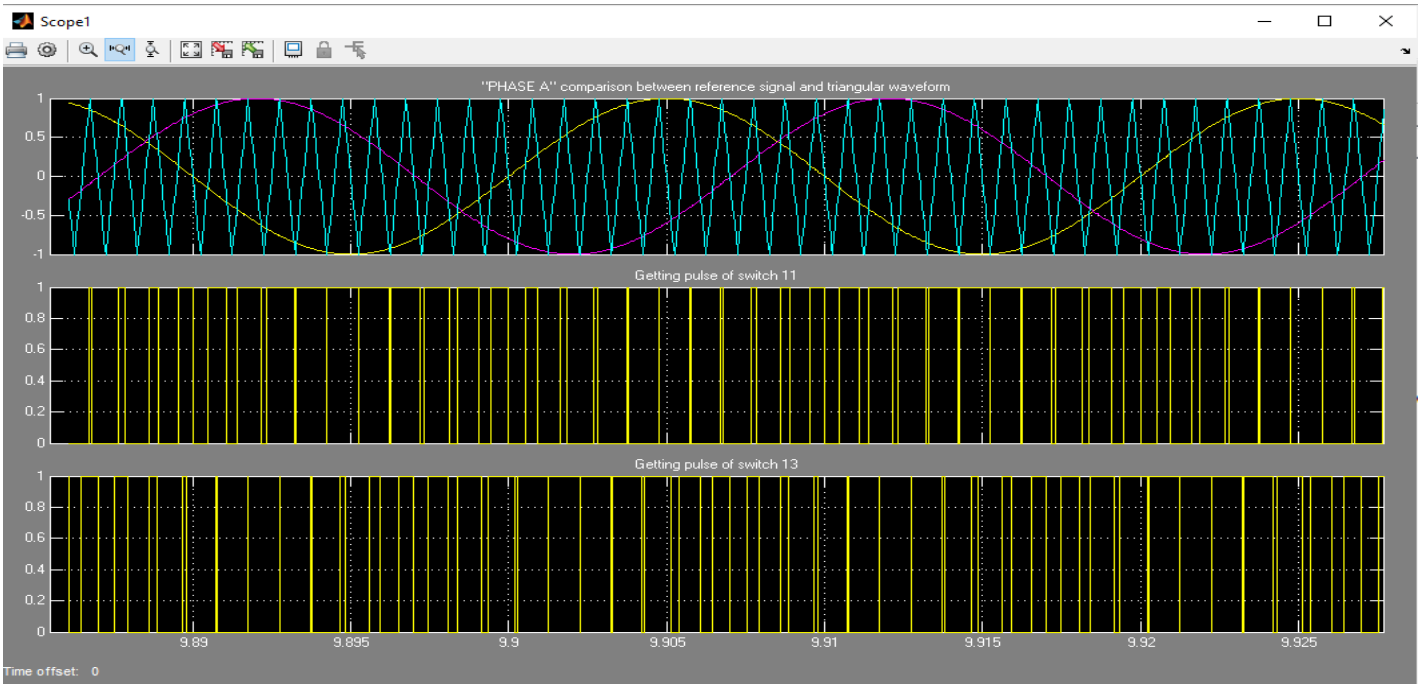


Figure 3.18 Unipolar PWM inverter waveforms output voltage and switching signals for phase A

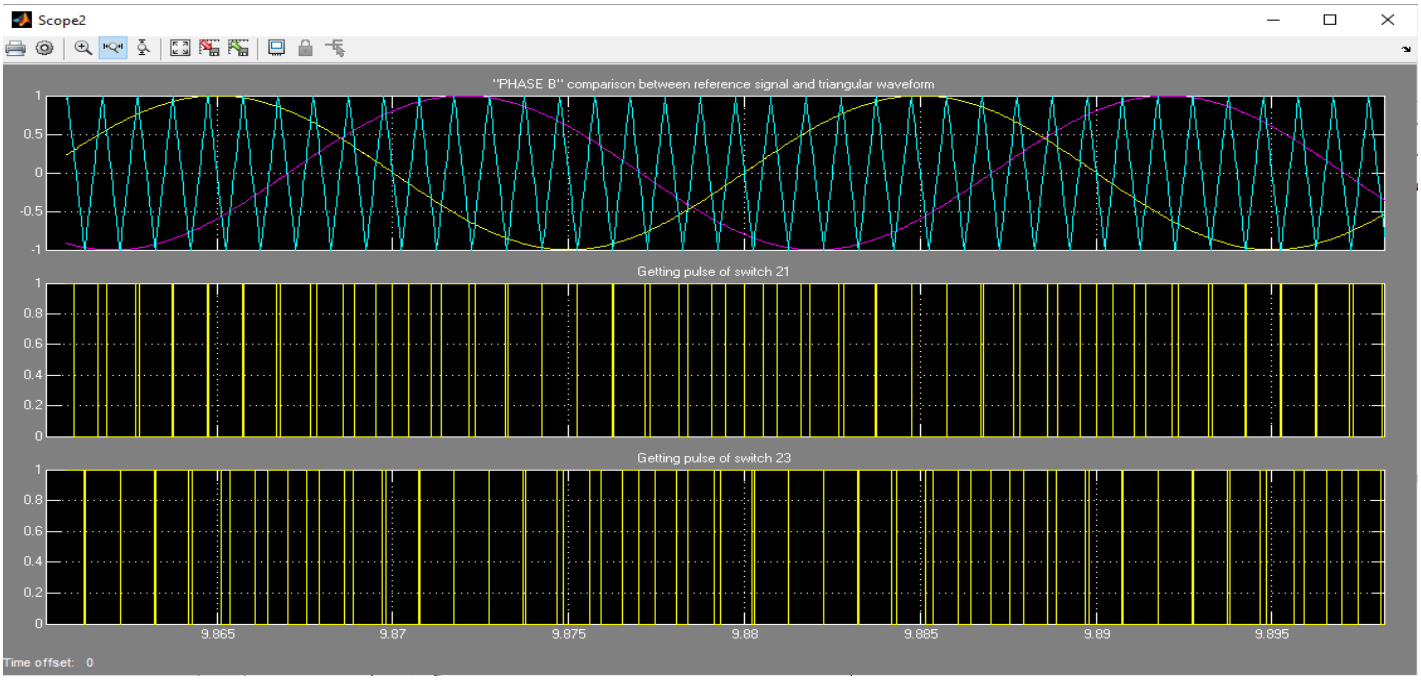


Figure 3.19 Unipolar PWM inverter waveform output voltage and switching signals for phase B

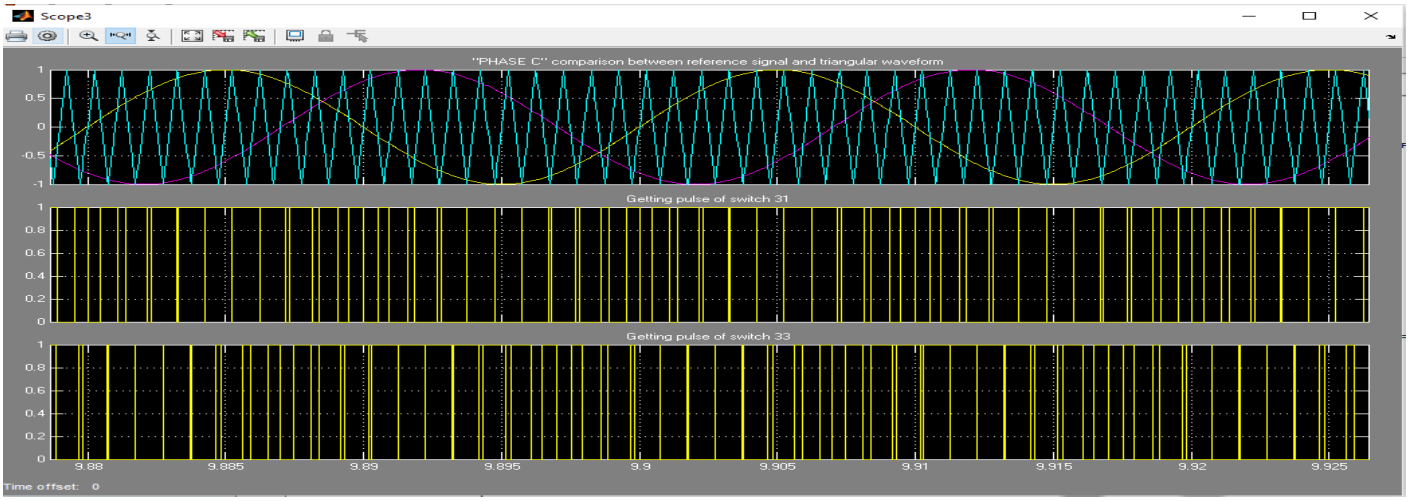


Figure 3.20 Unipolar PWM inverter waveforms output voltage and switching signals for phase C

CHAPTER 4

CONTROLLER DESIGN

4.1 Introduction

This topic will cover the design of a PI controller for an electric vehicle (EV) system's induction motor. Because PI control is a type of feedback control, it may enhance the performance of this IM system. Adding the proportionate action results in a quicker response time than the I-only control. PI control can stabilize the system, tune the inverter line to line voltage, and bring the system back to its predetermined position. The PI Controller is simulated using the MATLAB/Simulink program.

4.2 System Design

The initial step in developing a single-phase H-bridge inverter to control the induction motor was to create a mathematical model of the electric vehicle and induction motor. The following stage involved building three single-phase H-bridge inverters with PI controllers for an electric car system's induction motor. The proposed control system's block schematic was then created (see figure 4.1). The controller design has been tested using simulation in MATLAB/Simulink.

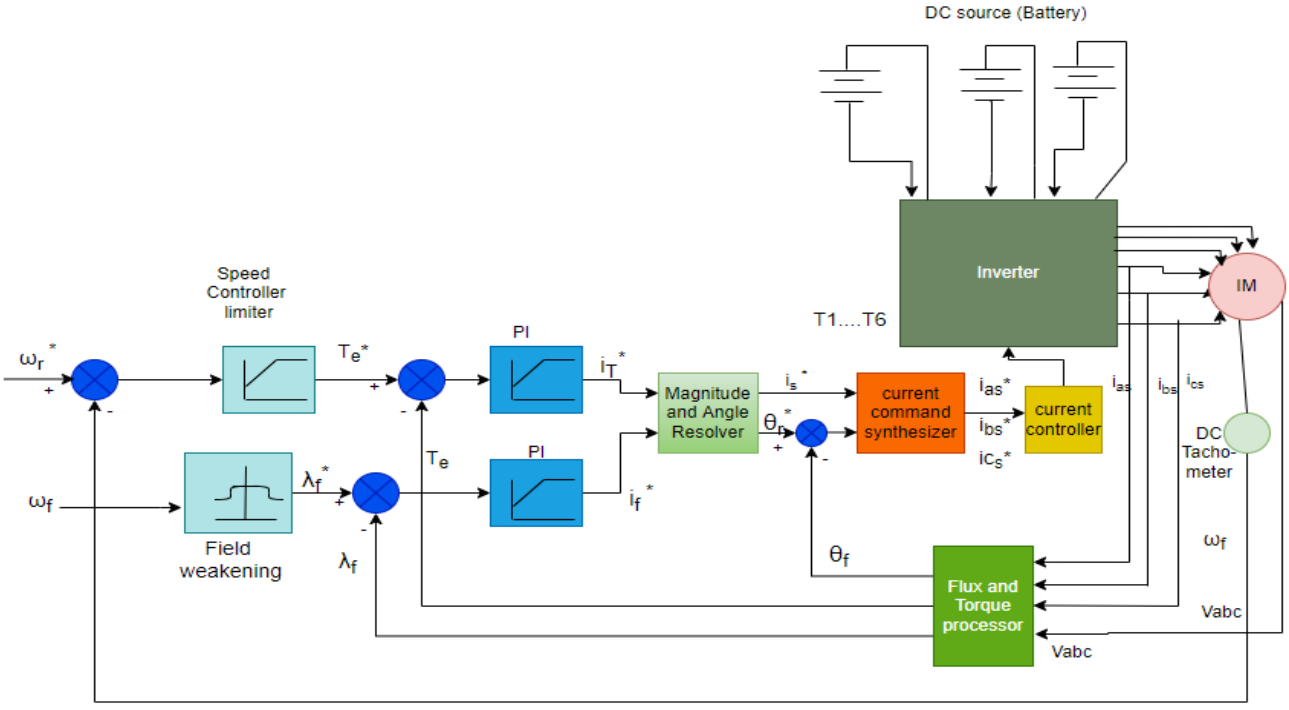


Figure 4.1 Block diagram of overall modeling system

The block diagram shown above shows the induction motor control system for an electric car with three single-phase H-bridge inverters. It also shows the planned PI controller, which is intended to regulate the power of each inverter feeding the OEWIM. According to the block diagram input, the stator flux and torque are controlled directly based on the instantaneous flux and torque error [23]. The output of a two-level PI controller is the error signal.

Typically, the flux between the stator and the rotor is kept at a constant amount, and the flux angle between them controls the motor torque. The switching strategy's cornerstone is the use of space vector modulation. A PWM adaptation improves the current profile of the inverter and lessens torque pulsation [23]. The produced torque T_d and stator flux vector λ_s are determined using v_s and i_s. The flux control loop compares the stator flux's magnitude, λ_s, to a reference value, λ_s*, and the torque, T_d, to a reference value, T_d*. The corresponding PI controllers are subjected to the flux and torque errors, $\Delta\lambda_s$ and ΔTd.

4.3 Controllers

In the most recent work, numerous modeling and regulating approaches for an electric vehicle system have been improved. To achieve the intended performance, a great model and a good control system are very essential.

4.4 Design PI Controller

There are numerous ways to create a PI controller. Ziegler-Nicholas design is possible in this study. It is possible to use the Toolbox in MATLAB/SIMULINK to acquire the precise values of kp and ki. Each PI controller can be created independently due to the decoupling of the voltage loop and current loop. The PI controller for the current loop can be built using the transfer function between the inductor current and the current reference. Twelve switches for each of the three single-phase H-Bridge inverters that are mentioned should be constructed in a way that requires the fewest number of switch transitions. An error signal is calculated by a PI

controller, a feedback control loop, by subtracting the system output from the set point.

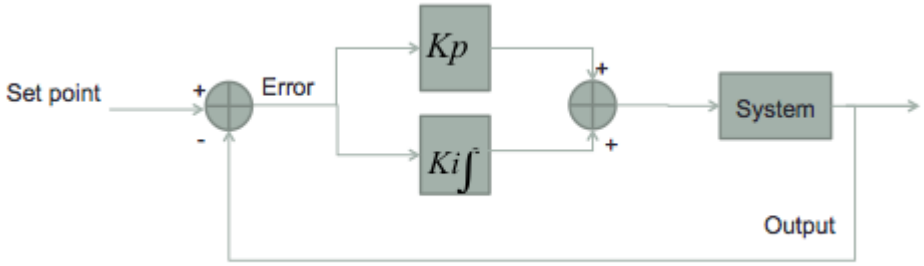


Figure 4.2 block diagram of PI controller

This is useful when integral control is required to lower the error that is constant over time and proportional control is required to accelerate the settling. A type of feedback control is PI control. Adding the proportionate action results in a quicker response time than I-only control. The system can be brought back to its set point via PI control, which also prevents the system from oscillating. Even while PI-control has a quicker response time than I-only control, P-only control is still up to 50% slower.

4.4.1 Proportional Controller

The control output of a proportional (P) controller (Figure 4.2) is inversely correlated with the error signal. The difference between the output (also known as the feedback signal) and the reference signal is known as the error signal. The control signal is amplified by a proportional controller. For a certain fault, the controller will exert more pressure, and the closed-loop system will swiftly respond by increasing overshoot. P controller does not eliminate the steady-state error, but it does reduce it. The dynamics of the closed loop can be altered by changing the control parameter Kp.

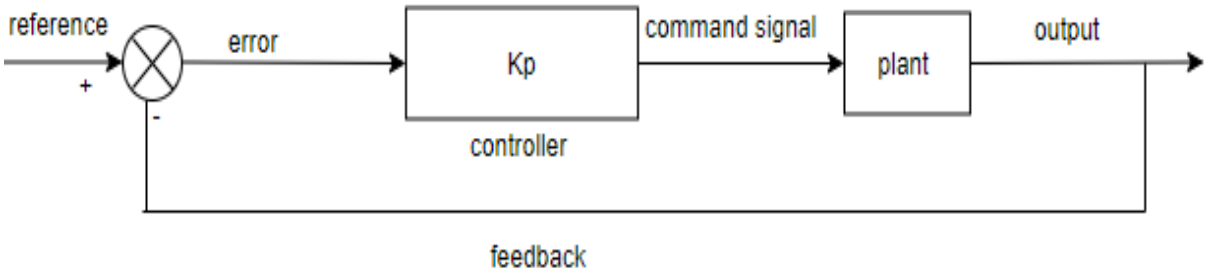


Figure 4.3 Proportional controllers in a feedback control loop.

4.4.2 Integral Controller

The response error history is used by the integral controller (Figure 4.3). The control signal is always that portion of the actuating-error-signal curve that is under the curve up until that point. As a result, even when the error signal is reduced to zero, the control signal u will still be non-zero. To construct the control signal, the region under the error signal before it became zero will be added [36]. Therefore, the offset error is removed using the integral controller. The integrator continuously builds, increasing the control signal and reducing the error when there is a persistent (constant) steady-state error. The control signal keeps getting stronger. Since it takes some time for the control signal to shift direction when the error signal changes sign, the integrated controller slows the system down and increases overshoot. The oscillations in the system cannot be eliminated by it. The integrated controller takes into account the response error history. The control signal at that specific moment is represented by the region under the actuating-error signal curve up to that point.

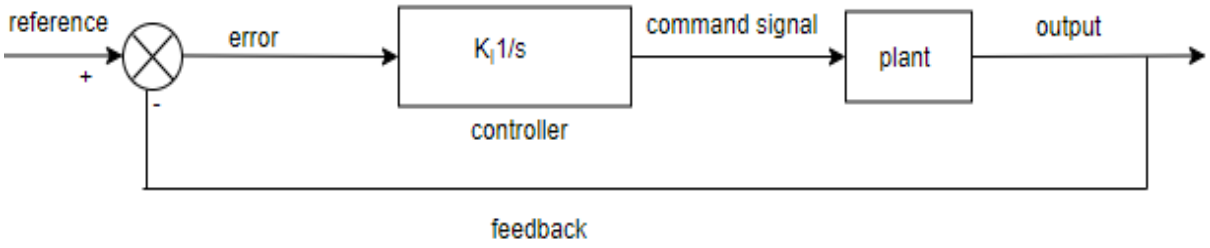


Figure 4.4 Integral gain block diagram

The offset error is removed using the integrated controller. The integrator continuously grows when there is a persistent (constant) steady-state error, raising the control signal and bringing the error down.

4.4.3 PI Controller

A type of feedback control is PI control [36]. Adding the proportionate action results in a quicker response time than I-only control. The system can be brought back to its set point via PI control, which also prevents the system from oscillating. Even while PI-control has a quicker response time than I-only control, P-only control is still up to 50% slower. The integral gain term is KI, while KP is the proportional gain term. In this simulation, the trial-and-error method is utilized to determine an appropriate number for KP and KI. The gains are initially set to 0, and then the values are gradually increased to a certain value until they reach a point where they are considered acceptable. Matlab software is then used to run the simulation. A mixture of the

outputs from the proportional and integral controllers is produced by the PI controller. Two distinct stable parameters are part of the PI controller. This controller has two terms. The P (Proportional component) denotes the error present estimation, whereas the I (Integral part) denotes the error's previous estimation. If the inaccuracy is greater, the proportional component will result in a higher output. Although it can shorten the rising time, it cannot eliminate the steady-state inaccuracy. As the gain is raised, the error will go down but the oscillations will go up. If the controller's output cannot minimize the mistake, the integral component will cause it to accumulate. Although the steady state error may be eliminated, the transient reaction becomes sluggish. With increasing integral time, oscillations become more pronounced.

The controller's performance can be shown in terms of how quickly it reacts to errors, how far it deviates from the set point, and the oscillations it causes. The output is so close to the set point because of the controller's actions. A PI controller is generally represented mathematically.

$$u(t) = k_P e(t) + k_I \int e(t) \tag{4.1}$$

Where; K_p is the proportional gain, K_i is integral gain, $\mathrm{u(t)}$ is set point and $\mathrm{e(t)}$ is an error

Let Substitute eq.4.1 to Laplace Transform on both sides

$$U(S) = k_P E(S) + k_I \frac{E(S)}{S} \tag{4.2}$$

$$U(S) = E(S)\left(k_P + \frac{k_I}{S}\right) \tag{4.3}$$

Therefore the transfer function of PI controller is:

$$\frac{U(S)}{E(S)} = k_P + \frac{k_I}{S} \tag{4.4}$$

Proportional Integral (PI) control is a technique used in almost all industrial control systems. Any system type can be coupled to the universal control calculation, which will provide stable control when adjusted properly. The most popular feedback controller is the PI controller [36]. Today, PI controllers can be found everywhere that uses control. Every control designer's toolkit must include it. It calculates the error and makes an effort to reduce it. Through the use

of control parameters, the sum of the two actions is used to alter the process. The output is controlled by the controller to be so close to the set point.

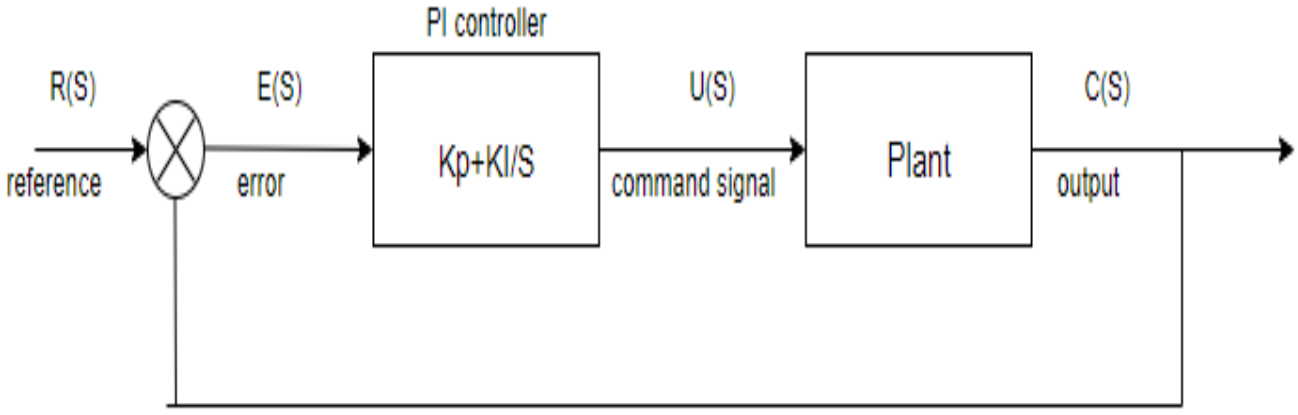


Figure 4.5 PI controllers in a feedback control loop.

Table 4.1 studying the differences between a step response for a second order system with a P and I controller.

Close-loop response	Rise Time	Overshoot	Settling time	Steady-state error
P controller	↓	↑	~	↓
I controller	↓	↑	↑	↓

4.5 Ziegler-Nichols Tuning

4.5.1 Ziegler–Nichols First Tuning Method

Then fine-tuning PID controllers for plants whose precise dynamics are unknown, Ziegler-Nichols (ZN) rules are widely employed; however, they may also be used with plants whose dynamics are known. In order to calculate proportional gain Kp and integral time Ti values based on the transient response characteristics of a particular plant, Ziegler and Nichols provided guidelines [36].

The first approach is used with plants that exhibit step responses in the form shown in table 4.1. This kind of response is typical of a first-order system, like the one brought on by fluid flow. Additionally, it is indicative of a first-order system-based plant. L, the delay time, and T, the time constant, are the two parameters that define the response. Based on this model, Ziegler and Nichols deduced the following control parameters.

Table 4.2 - Ziegler-Nichols Recipe – First Method

PI type	Kp	$T_i = \frac{K_p}{K_i}$
P	$\frac{T}{L}$	∞
PI	$0.9\frac{T}{L}$	$\frac{L}{1.3}$

4.5.2 Ziegler–Nichols Second Method

The second approach is to control plants that might become unstable under proportional control. This method necessitates the usage of the PI controller, hence it must be applied in a closed loop system. The following are the steps for fine-tuning a PI controller using the second approach:

Using only proportional feedback control:

- ✓ Set the Integrator and Derivative Gains to 0;
- ✓ Raise Kp from a low value to a critical value at which oscillations occur, where Kp = Kcr. A different approach must be used if it doesn't happen.
- ✓ Take note of the value Kcr and the equivalent period of sustained oscillation, Pcr. It is important to note that the oscillations must have an equal duration in order for them to be applied.

The following is currently a list of the controller gains:

Table 4.3 Ziegler Nichols Formula – Second Method

PI type	Kp	Ti
P	$0.5Kcr$	∞
PI	$0.45Kcr$	$\frac{p_{cr}}{1.2}$

CHAPTER 5

SIMULATION RESULTS AND DISCUSSION

5.1 Subsystem of system design description

The overall system simulated with matlab Simulink toolbox. PI controller to regulate the torque and flux linkage in the inner loop. Simulation results are presented and analyzed to illustrate the feasibility of the proposed voltage of induction motor control system for electric vehicle parameter estimators. Figure 5.1 is the the overall scheme of the induction motor for electric vehicle.

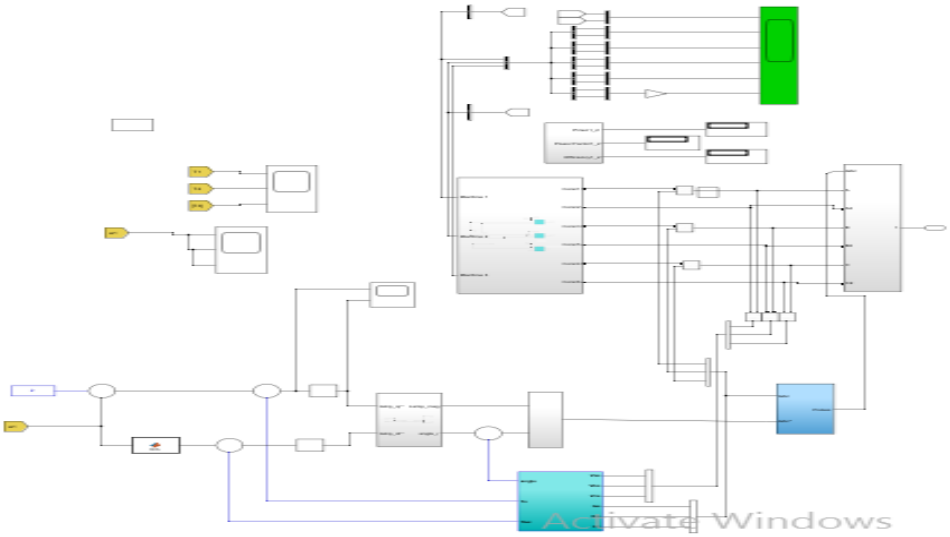


Figure 5.1 Proposed PI control scheme for induction motor of electric vehicle and overall model of system design

Since six terminal three-phase induction motor is not available in the Matlab Simulink toolbox three single-phase motors are used for simulation. The three H-bridge converters are connected with each motor's phase windings. The output filter inductor is not necessary as the inductance of the phase winding is used as the output filter . one of the problems of the vehicle system is the circulation of current in battery modules. This model, it requires 21 series and 50 parallel, models. To avoid the circulation of current between battery modules separate converters are proposed in this thesis. This avoids the circulation current from phase A dc-link to phase C and B and vice versa.

5.2 Stator Voltage and current sensors

The three-phase voltages are measured through voltage sensors. However, to avoid the zero sequence due to an unbalanced system one-third of the neutral voltage is added to each phase voltage. A similar action is done in the current as is shown on the leftmost in figure 5.2.

$$v_{qs}^{s} = v_{as} \tag{5.1}$$

$$v_{ds}^{s} = -\frac{1}{\sqrt{3}} v_{bs} + \frac{1}{\sqrt{3}} v_{cs} \tag{5.2}$$

Similar to how the voltages are determined; these equations also apply to the currents. The stator equations for the induction motor are derived from the stator reference frame equations.

$$v_{qs} = (R_s + L_s P) i_{qs} + L_m P i_{qr} \tag{5.3}$$

$$v_{ds} = (R_s + L_s P) i_{ds} + L_m P i_{dr} \tag{5.4}$$

From which the rotor currents i_{qr} and i_{dr} can be computed as

$$i_{qr} = \frac{1}{L_m} \left\{ \int (v_{qs} - R_s i_{qs}) dt - L_s i_{qs} \right\} \tag{5.5}$$

$$i_{dr} = \frac{1}{L_m} \left\{ \int (v_{ds} - R_s i_{ds}) dt - L_s i_{ds} \right\} \tag{5.6}$$

The following formulas can be used to calculate torque, flux, and field angle from all the stator and rotor currents.

$$T_e = \frac{3}{2}\frac{P}{2} L_m (i_{qs} i_{dr} - i_{ds} i_{qr}) \tag{5.7}$$

$$\lambda_{qr} = L_r i_{dr} + L_m i_{ds} \tag{5.8}$$

$$\lambda_{dr} = L_r i_{qr} + L_m i_{qs} \tag{5.9}$$

$$\lambda_r = \sqrt{(\lambda_{qr})^2 + (\lambda_{dr})^2} \tag{5.10}$$

$$\theta_f = \tan^{-1}\left(\frac{\lambda_{qr}}{\lambda_{dr}}\right) \tag{5.11}$$

Computational circuits can be used to implement the equations given above, as seen in figure 3.19. The development of code for implementation in a single chip processor might be done using the same diagram. Note how the motor parameters Rs, Ls, Lr, and Lm affect the circuit. The stator resistance variations could be indirectly monitored using cheap temperature sensors. Due to the use of flux regulation, the inductances in this system wouldn't undergo any appreciable changes. As a result, the accuracy of the measurement and calculation of flux, torque, and field angle would not be significantly affected by parameter sensitivity.

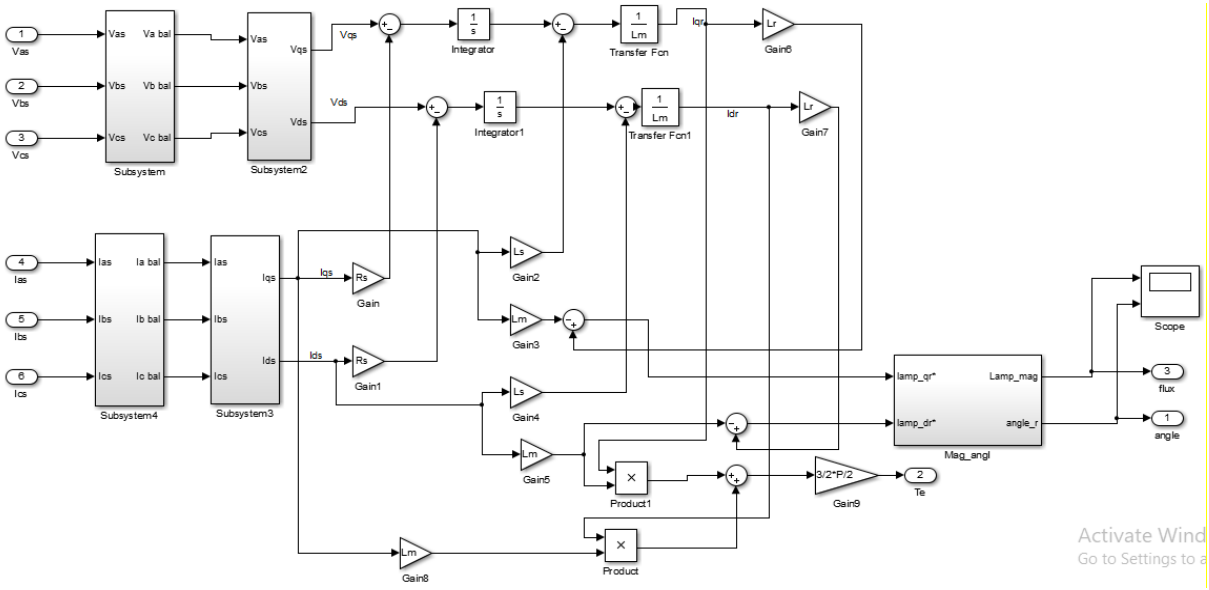


Figure 5.2 flux and torque processor implementation

5.3 Stator flux-based calculator

The number of calculation steps and the reliance on numerous motor parameters may be considerably reduced by employing the stator flux links and computing the electromagnetic

torque using only the stator flux linkages and stator currents. For just resistance is used, the mutual and rotor inductances of the machine are not dependent on the application when computing the stator flux linkages. The following is a basic summary of the steps involved:

$$\lambda_{ds} = \int (v_{ds} - R_s i_{ds})\, dt \tag{5.12}$$

$$\lambda_{qs} = \int \left(v_{qs} - R_s i_{qs}\right) dt \tag{5.13}$$

$$\lambda_s = \sqrt{(\lambda_{qs})^2 + (\lambda_{ds})^2 < \theta_{fs}} \tag{5.14}$$

$$\theta_{fs} = \tan^{-1}\left(\frac{\lambda_{qs}}{\lambda_{ds}}\right) \tag{5.15}$$

$$T_e = \frac{3}{2}\frac{P}{2}\,(i_{qs}\lambda_{ds} - i_{ds}\lambda_{qs}) \tag{5.16}$$

In this case the flux loop can be closed with the stator flux linkages instead of the rotor flux linkages.

5.4 Magnitude to Angle subsystem

The value of the subsystem input at the previous time step is produced for Triggered Subsystems by "Latch input by delaying outside signal," given a model or subsystem input ports. When the "Latch input for feedback signals of function-call subsystem outputs" is "On," the input value to the function-call subsystem cannot change while it is in operation. The additional parameters can be utilized to explicitly characterize the characteristics of the input signal.

The real Imaginary to Complex method involves creating a complex output from real and/or imaginary input. When real-imaginary to complex's output is provided as input, the complex to magnitude angle is employed to calculate the magnitude and/or radian phase angle of the input. Give a model or subsystem an output port as a last step. The "Output when deactivated" and "Initial output" options only apply to subsystems that are used in specific situations. The output of a subsystem that is conditionally run is either preserved at its prior value or changed to "Initial output" when it is disabled..

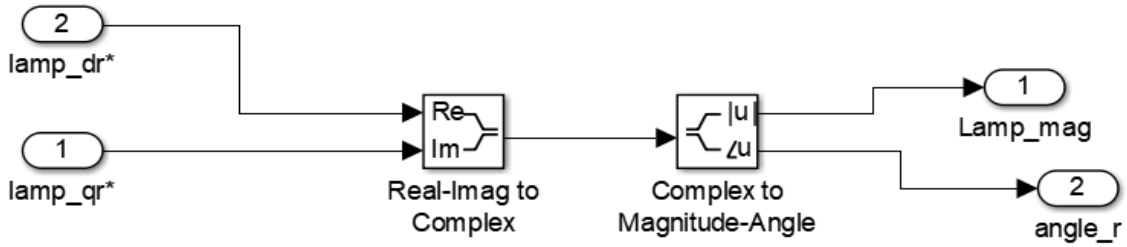


Figure 5.3 magnitudes to angle conversation

5.4.1 dq to abc conversation

This system is used to convert two inputs (Teta_s and Is*) using multiplex to three different currents (Is_abc*). In the block model for a synchronous machine, where the stator values are coupled to the rotor, the dq to abc Transformation block is utilized. Once the values for the stator and rotor are referred to a fixed or rotating reference frame, the Park transformation is performed to remove time-varying inductances. The Id and Iq currents, which run in two equivalent rotor windings and give the same flux as the Ia, Ib, and Ic currents in the stator, are two DC currents (d winding on the same axis as the field winding and q winding in quadratic).

Dq: Connect a vectorized signal comprising the sequence components [d q 0] to be transformed to the first input.

Sin cos: Connect a vectorized signal with the values [sin(ωt) cos(ωt)], where is the rate of rotation of the reference frame, to the second input.

abc: The output is a vectorized signal that has the same units as the dq0 input signal and contains the three-phase sinusoidal values [phase A, phase B, and phase C].

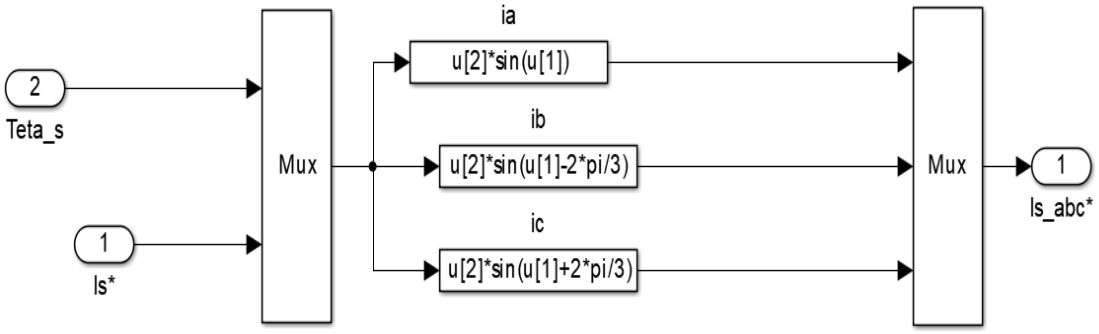


Figure 5.4 dq to abc conversation

5.5 Current regulator

A device that transforms current detected in an induction motor system into a physical signal proportionate to the current for each three phases is what the Current Regulator Block represents as an ideal current sensor. The sensor is connected to the circuit using connections + and -, which are electrically energy-saving ports. A physical signal port called Connection I is where the measurement's outcome is output. Various Simulink/Block components are used in this section to control a system's current flow, including Relay used to compare the input to the designated thresholds and output the appropriate "on" or "off" value. The input between the upper and lower limits has no effect on the relay's on/off state.

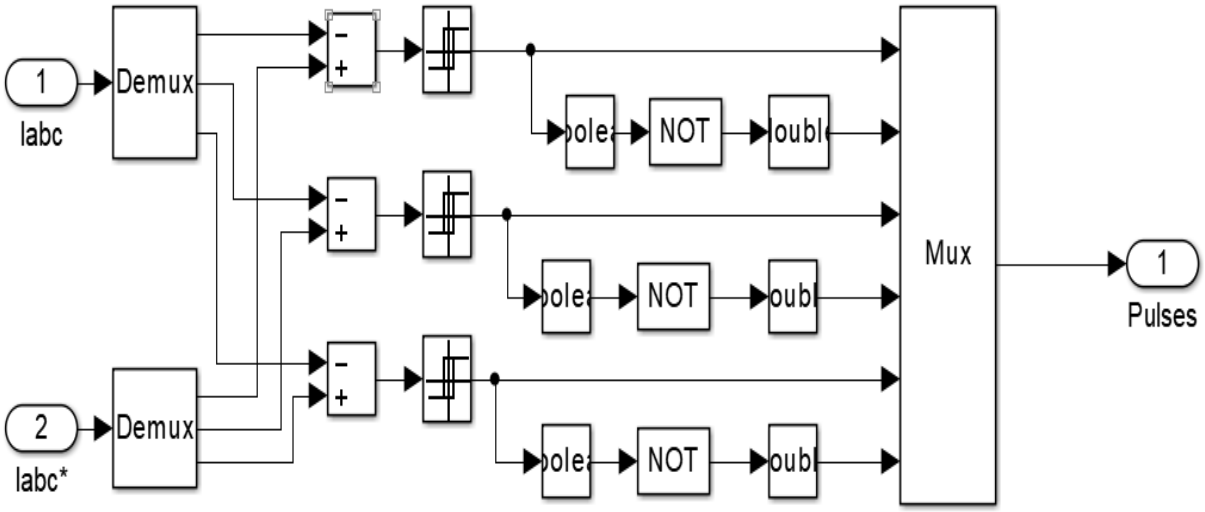


Figure 5.5 current regulators

5.6 Simulation result of the system design

First,using MATLAB/SIMULINK, the performance of the three single-phase H-Bridge inverters supplied IM drive is investigated. The developed inverter architecture is based on insulated gate bipolar transistor (IGBT). Table 3.1 lists the three-phase OEWIM's parameters. Examination of PWM The OEWIM is first driven using the PWM1 switching sequence. 148 V is the applied dc-link voltage.Figure 5.7 demonstrates the flux and torque simulation data needed for an induction motor. The OEWIM has a 5.4Ah battery capacity, with a battery voltage of 7.2V for each cell, and is powered by separate single-phase H-Bridge inverters coupled to

equal dc-link voltages. IGBTs were used in the construction of this inverter to convert the provided dc power to the AC source needed for the electric vehicle motor. In this system, 50 battery cells are linked in parallel with 21 series-connected cells, hence 1050 battery cells are intended for this system.

5.6.1 PI Controllers' performance on torque and flux

There are two parameters, Kp and Ki, in this PI controller approach. It is suggested to adjust PI settings using the Ziegler Nichols approach. By using the first and second Ziegler Nichols methods to obtain the PI parameter result, we may change the PI value based on the simulation results to obtain the optimal parameter values.

The system may begin oscillating if the Kp value is increased (too much), and if it is decreased (too little), the system may become less responsive and fail to react. It reacts to pass values for the Ki value in order to exceed the set point. Ki removes the lingering steady-state error.

5.6.2 Three phase Current

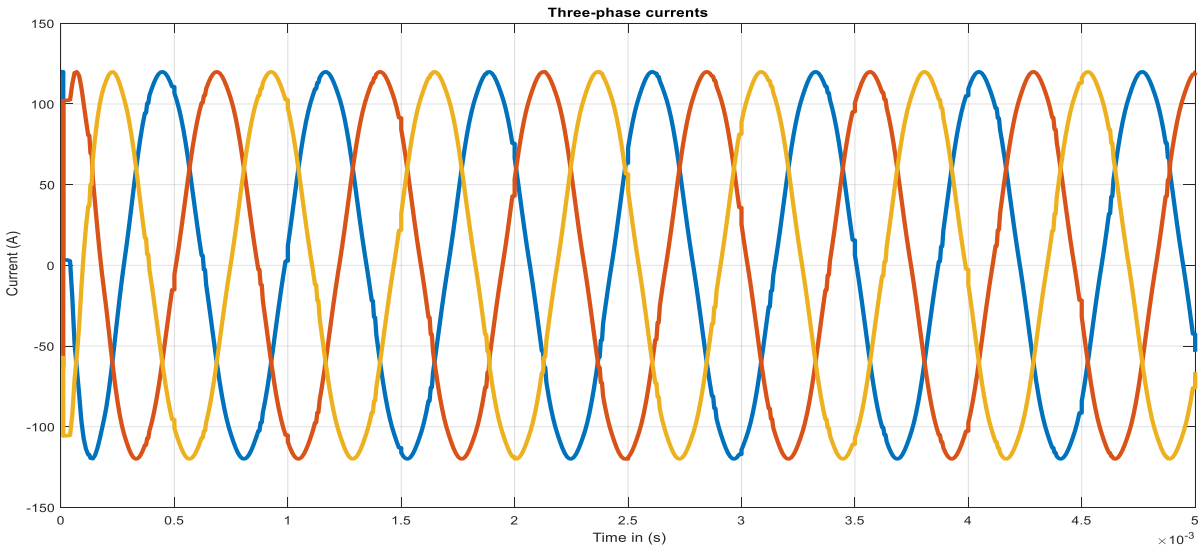


Figure 5.6 Step responses of Three-phase current in (A)

5.6.3 Torque of the motor

A PI controller is used to regulate the speed of the electric vehicle as well as the induction motor's torque. Strong torque at zero speed, high-speed cruising (field weakening), and the

ability to run at a slightly variable DC battery voltage level are all requirements for electric vehicles. The outcome of a simulation with a 0.7 sample time and a 733 final value Once the motor has been running for a while, the time response progressively increases to reaches the maximum overshoot after then its gradually its becoming steady state. The EV motor's torque is controlled by PI, with the parameters chosen being 1.464, 1672.89 respectively. The speed of the troque loop is 10 times faster than the speed loop. The speed loop is design for 25 rad per second.

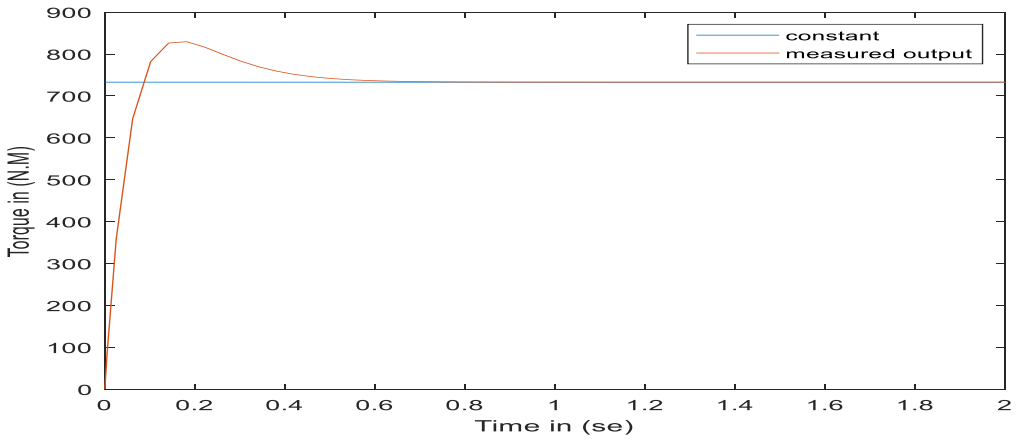


Figure 5.7 Step responses of torque

5.6.4 Flux

A PI controller is used to regulate the induction motor's flux as well as the speed of the electric vehicle. The outcome of a simulation with a 1.5 sample time and a 150 final value The EV motor flux is controlled using PI, and the parameters used for PI are 1.46448, and 1672.89 respectively.

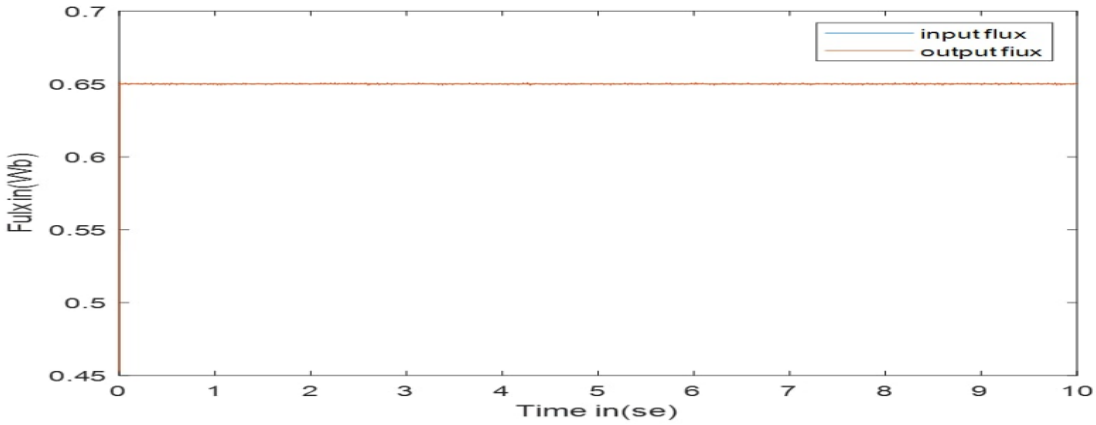


Figure 5.8 Step responses of flux

5.6.5 Angle

The angle of motor is converted from the magnitude, and the time response of the system become to steady state after the overshoot of 120 rad/s then its gradually decrease to settling point.

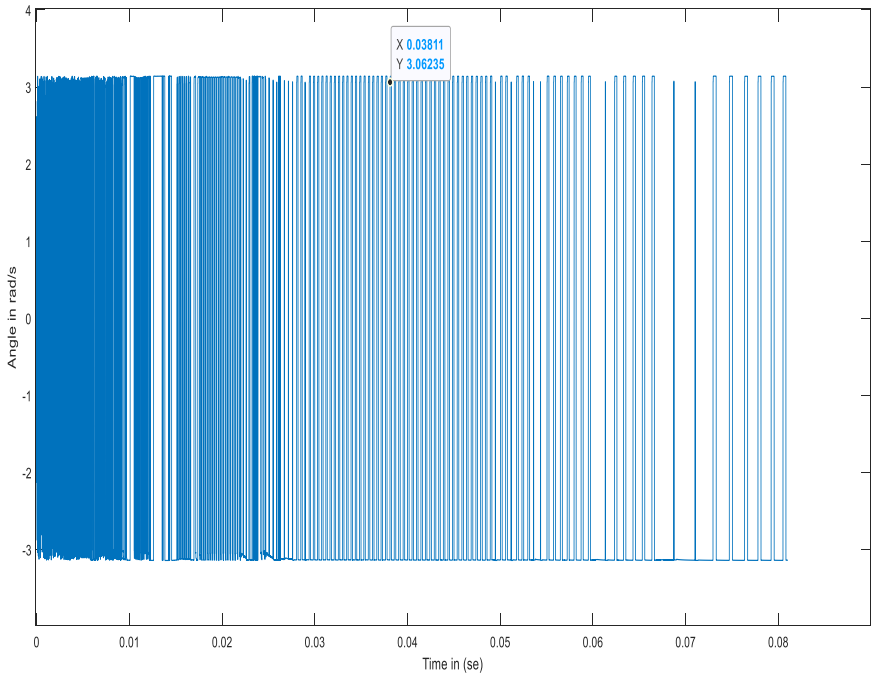


Figure 5.9 Step responses of Angle

CHAPTER 6
CONCLUSION AND FUTURE SCOPE

6.1 Conclusion

High power density IM in EV uses a lot of battery electricity. Numerous batteries are linked in parallel to meet these current demands and individual battery current limits. A circulating current begins to flow between parallel-connected batteries when there is a terminal voltage differential between them, which m shorten the life of the battery. As the number of the parallel path increases the circulation current also increases.

Each phase winding of the OEWIM is supplied through a single-phase H-Bridge inverter in order to decrease the number of parallel-connected batteries. PWM is used to create and assess a unipolar inverter for CMV. The control torque and flux used by the PI controller approach to send input to the system are evaluated.` The proposed strategy has been also verified and run through simulation on Matlab/Simulink software.

6.2 Future of the study

By combining other controllers like adaptive controllers and evolutionary algorithms for the tuning of PI controllers, this work on EV motor control can be expanded. Different situations may be used to evaluate the functioning of the controller to control the performance of the EV motor. The proposed approach may use an algorithm, and the performance may be compared or improved outcomes may be attained. One of the issues is the computing time of the algorithm, and related research might be expanded to find ways to shorten it. On top of that, the research also will verify with a practical experiment using the Texas instrument in the future.

REFERENCES

[1] Sreenath, M., and S. Indulal. "Design and Analysis of a Fuzzy Logic Controller for the Optimal Switching of Drives for Hybrid Electric Vehicles," *International Conference on Control Communication & Computing India (ICCC),* pp. 84–89.IEEE, 2015.

[2] Tolbert, Leon M., Fang Z. Peng, and Thomas G. Habetler. "Multilevel Inverters for Electric Vehicle Applications." In *Power Electronics in Transportation (Cat. No. 98TH8349)*, pp. 79-84. IEEE, 1998.

[3] F. Roemer, M. Ahmad, F. Chang, and M. Lienkamp, "Optimization of a Cascaded H-Bridge Inverter for Electric Vehicle Applications Including Cost Consideration,"no.22 pp. 1–19, 2019, doi: 10.3390/en12224272.

[4] D. Wang, L. Piegari, D. De Simone, and X. Chen, "A Battery Lifetime Improved Control Strategy of Modular Multilevel Converter for Electric Vehicle Application," *2019 IEEE 10th Int. Symp.* Power Electron. Distrib. Gen*er. Syst.*, no. 978, pp. 594–598, 2019.

[5] Vodovozov, Valery, Nikolai Lillo, and Zoja Raud. "Single-Phase Electric Drive for Automotive Applications." In *2014 International Symposium on Power Electronics, Electrical Drives, Automation and Motion*, pp. 1313-1318. IEEE, 2014.

[6] M. J. Akhtar, R. K. Behera, and S. Member, "Space Vector Modulation for Distributed Inverter Fed Induction Motor Drive for Electric Vehicle," vol. 6777, no.1 pp. 1–11, 2020, doi: 10.1109/JESTPE.2020.2968942.

[7] K. Abdelfatah *et al.*, "Space Vector PWM Control Synthesis for a H-Bridge Drive in Electric Vehicles To cite this version : Space Vector PWM Control Synthesis for a H-Bridge Drive in Electric Vehicles," *IEEE Transactions on Vehicular Technology*, no 6.pp.2441-2452. 2013.

[8] W. Cai, X. Wu, M. Zhou, Y. Liang, and Y. Wang, "Review and Development of Electric Motor Systems and Electric Powertrains for New Energy Vehicles," *Automot. Innov.*, vol. 4, no. 1, pp. 3–22, 2021, doi: 10.1007/s42154-021-00139-z.

[9] Akshaya, S. R., and SG Bharathi Dasan. "Cascaded h bridge inverter motor drive for electric vehicle applications."vol 2. no. 3.pp16-22, 2016.

[10] F. Chang, "Modelling and Evaluation of Battery Packs with Different Numbers of Paralleled Cells,"World Electric Vehicle Journal, 9(1), pp.8, 2018, doi: 10.3390/wevj9010008.

[11] Narender Reddy, K. and Pradabane, S., "Modified H-bridge inverter based fault-tolerant multilevel topology for open-end winding induction motor drive," *IET Power Electronics*, *12*(11), pp.1-11, 2019. doi: 10.1049/iet-pel.2018.6061.

[12] G. Renukadevi and K. Rajambal, "Modeling and Analysis of Multi-Phase Inverter Fed Induction Motor Drive with Different Phase Numbers 2 D-Q Model of 5-Phase Induction Motor Drive," vol. 8, no. 3, pp. 73–80, 2013.

[13] O. Josefsson, *Investigation of a Multilevel Inverter for Electric Vehicle Applications*. 2015.

[14] M. Ahsan, N. Ahmed, and M. Hussain, "A Comparative Study of Controllers for Optimal Speed Control of Hybrid Electric Vehicle," In2016 International Conference on Intelligent Systems Engineering (ICISE), no. 3, pp. 8–11, 2016.IEEE.

[15] M. V. Sarin, A. Chitra, P. Sanjeevikumar, and A. Venkadesan, "Induction Motor Control Schemes for Hybrid Electric Vehicles/Electric Vehicles," *Artif. Intell. Tech. Electr. Hybrid Electr. Veh.*, pp. 165–178, 2020, doi: 10.1002/9781119682035.ch9.

[16] M. J. Akhtar and R. K. Behera, "Optimal design of stator and rotor slot of induction motor for electric vehicle applications," pp. 1–9, 2018, doi: 10.1049/iet-est.2018.5050.

[17] Z. Wu and E. Engineering, "Energy Efficient PWM Induction Machine Drives for Electric Vehicles," University of Sheffield, 1999.

[18] M. M. Haleth, R. P. Kumar, and J. J. Priska, "Cascaded Multilevel Inverter for Hybrid," pp. 116–124, 2016.

[19] I. T. Salsabil, "design and implementation of a single phase symmetrical hybrid sinusoidal pulse width design and implementation of a single phase symmetrical hybrid sinusoidal pulse width," no. November, 2016.

[20] A. T. Sowmya, "Design And Implementation Of PI And PR Current Controllers For Smart Inverter."

[21] Maswood AI. A PWM voltage source inverter with PI controller for instantaneous motor current control. In Proceedings of International Conference on Power Electronics and Drive Systems. PEDS 95 (pp. 834-837), IEEE,1995 .

[22] T. C. A. Ajot, S. Salimin, and R. Aziz, "Application of PI Current Controller in Single Phase Inverter System Connected to Non Linear Load," *IOP Conf. Ser. Mater. Sci. Eng.*,

vol. 226, no. 1, 2017, doi: 10.1088/1757-899X/226/1/012135.

[23] S. M. Cherati, N. A. Azli, S. M. Ayob, and A. Mortezaei, "Design of a Current Mode PI Controller for a Single-phase PWM Inverter," In *2011 IEEE Applied Power Electronics Colloquium (IAPEC)*, pp. 180–184, 2011.

[24] S. Sivaganesan, C. Somasankarappa, and P. V. S. Aditya, "Modeling of Direct-Quadrate (D-Q) of 3 Phase Induction Motor using MATLAB / SIMULINK Page No : 619," vol. 7, no. 2236, pp. 619–631, 2018.

[25] J. Mei *et al.*, "Modeling and Optimizing Method for Axial Flux Induction Motor of Electric Vehicles c," vol. 9545, no.11. 2020, doi: 10.1109/TVT.2020.3030280.

[26] S. Member and N. C. Kar, "a survey and comparison of characteristics of motor Gaurav Nanda University of Windsor , Canada Converteric MoCool," no. May, pp. 1–4, 2006.

[27] P. N. Bhatt, H. Mehar, and M. Sahajwani, "Electrical Motors for Electric Vehicle – A Comparative Study," 2019.

[28] E. Theses and S. Ali, "Office of Graduate Studies an overview on why electric cars are the future of transportation," 2021.

[29] C. Paper, M. S. Kumar, and N. V. Bharadwaj, "Induction motor design analysis for electric vehicle application," no.1 November 2021, 2020, doi: 10.1063/5.0019486.

[30] S. Muehleck, "Design and Simulation of Interconnected H-Bridge Inverter By," 2012.

[31] A. Emadi, Handbook of Automotive Power Electronics and Motor Drives Edited . CRC press, 2017.

[32] S. Shah, A. Rashid, and M. K. L. Bhatti, "Direct Quadrate (D-Q) Modeling of 3-Phase Induction Motor Using MatLab / Simulink," vol. 3, no. 5, 2012.

[33] G. Abdalrahman, O. H. Abdalla, M. I. Jibril, and A. A. Awad, "Space Vector Pulse Width Modulation Technique Applied to Two Level Voltage Source Inverter," vol. 1, no. 2, pp. 10–17, 2018.

[34] X. Z. Qiu and G. R. Zhang, "Design and Research of the H-bridge inverter system Based on IGBT Design and Research of the H-bridge inverter system Based on," 2022, doi: 10.1088/1742-6596/2290/1/012055.

[35] E. H. Aboadla, S. Khan, M. H. Habaebi, and T. S. Gunawan, "Selective Harmonics Elimination Technique in Single Phase Unipolar H-Bridge Inverter," In *2016 IEEE Student Conference on Research and Development (SCOReD)*, pp. 1-4. IEEE, 2016.no.

December, 2016, doi: 10.1109/SCORED.2016.7810057.

[36] V. V. Patel, "Ziegler – Nichols Tuning Method ∗," vol. 25, no. 10, pp. 1385–1397, 2020.

[37] S. K. Vempalli, J. Ramprabhakar, S. Shankar, and G. Prabhakar, "Electric Vehicle Designing , Modelling and Simulation," In *2018 4th International Conference for Convergence in Technology (I2CT)* pp. 1–6, IEEE .2018.

[38] I. V. A. Veiga, R. Zymler, R. A. Shayani, D. M. Viana, and M. V. M. Orrico, "Sizing of Motor and Battery Pack for an Automotive Electric Vehicle Given a Specific Route," *2012 Sixth IEEE/PES Transm. Distrib. Lat. Am. Conf. Expo.*, no. March 2020, pp. 1–8, 2012, doi: 10.1109/TDC-LA.2012.6522595.